ADVANCED TRANSDUCER TECHNOLOGY
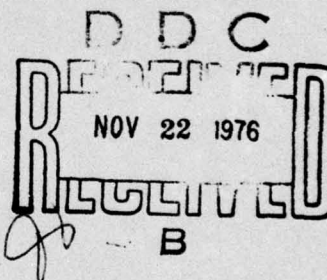Polyvinylidene Fluoride Transducer Technology

Southwest Research Institute

D D C

NOV 22 1976

RECEIVED

B

**ROME AIR DEVELOPMENT CENTER
AIR FORCE SYSTEMS COMMAND
GRIFFISS AIR FORCE BASE, NEW YORK 13441**

AD A032315

This report has been reviewed by the RADC Information Office (OI) and is releasable to the National Technical Information Service (NTIS). At NTIS it will be releasable to the general public including foreign nations.

This report has been reviewed and is approved for publication.

APPROVED: *Robert B. Curtis*

ROBERT B. CURTIS
Project Engineer

APPROVED: *Joseph L Ryerson*

JOSEPH L. RYERSON
Technical Director
Surveillance Division

FOR THE COMMANDER: *John P. Huss*

JOHN P. HUSS
Acting Chief, Plans Office

Do not return this copy. Retain or destroy.

REPORT DOCUMENTATION PAGE		READ INSTRUCTIONS BEFORE COMPLETING FORM
1. REPORT NUMBER RADC-TR-76-286-Vol-1 (of two)	2. GOVT ACCESSION NO.	3. RECIPIENT'S CATALOG NUMBER
4. TITLE (and Subtitle) ADVANCED TRANSDUCER TECHNOLOGY. Volume I. Polyvinylidene Fluoride Transducer Technology.		5. TYPE OF REPORT & PERIOD COVERED Final Technical Report 9 April 1975 — 9 June 1976
		6. PERFORMING ORG. REPORT NUMBER N/A
7. AUTHOR(s) Wendell R. Peters		8. CONTRACT OR GRANT NUMBER(s) F30602-75-C-0158
9. PERFORMING ORGANIZATION NAME AND ADDRESS Southwest Research Institute 8500 Culebra Road San Antonio TX 78284		10. PROGRAM ELEMENT, PROJECT, TASK AREA & WORK UNIT NUMBERS 62702F 6515132D
11. CONTROLLING OFFICE NAME AND ADDRESS Rome Air Development Center (OCDS) Griffiss AFB NY 13441		12. REPORT DATE September 1976
		13. NUMBER OF PAGES 62
14. MONITORING AGENCY NAME & ADDRESS(if different from Controlling Office) Same		15. SECURITY CLASS. (of this report) UNCLASSIFIED
		15a. DECLASSIFICATION/DOWNGRADING SCHEDULE N/A

16. DISTRIBUTION STATEMENT (of this Report)

Approved for public release; distribution unlimited.

17. DISTRIBUTION STATEMENT (of the abstract entered in Block 20, if different from Report)

Same

18. SUPPLEMENTARY NOTES

RADC Project Engineer: Robert B. Curtis (OCDS)

19. KEY WORDS (Continue on reverse side if necessary and identify by block number)

Transducer	Sensors
Polymer Film	Infrared
Pyroelectric	Imaging
Piezoelectric	

20. ABSTRACT (Continue on reverse side if necessary and identify by block number)

Various techniques were investigated for fabricating single element and multiple element pyroelectric detectors from polyvinylidene (PVF_2) films. Effort was applied towards the fabrication of vacuum deposited metal electrodes on the surface of the film. The best quality films were made with 100 to 1000 A° aluminum electrodes. Various techniques were used for poling the films to make pyroelectric devices. During the poling process, high voltage breakdown sometimes occurred due to imperfections in the film or was caused by pressure points

DD FORM 1473 EDITION OF 1 NOV 65 IS OBSOLETE
1 JAN 73

from the supporting apparatus which caused a dielectric weakening of the film. Successful fabrication techniques were achieved for both single element and multiple element detector arrays.

The single element detectors were used to investigate the pyroelectric effect and for the construction and testing simple infrared detectors. The multiple element detectors were designed to be used in a low resolution (4 x 4) infrared imaging instrument. The multiple element detectors were utilized in a bread-board model of an infrared imager which demonstrates the feasibility of the concept. The resulting instrument which used spherical reflecting mirrors as optics, was capable of detecting a human at approximately 5 meters.

ACCESSION for

NTIS	White Section	☑
DDC	Buff Section	☐
UNANNOUNCED		☐
JUSTIFICATION		

BY
DISTRIBUTION/AVAILABILITY CODES

| Dist. | AVAIL. and/or SPECIAL |

A

POLYVINYLIDENE FLUORIDE TRANSDUCER TECHNOLOGY
STUDIES FOR SECURITY SYSTEMS

PVF_2 Film Paper -- Outline

EVALUATION

This effort demonstrated the feasibility of adapting the pyroelectric capability of a polymer film material to an IR detector. The specific film, polyvinylidene fluoride, is an inexpensive rugged material which offers promise of yielding low cost, low powered, and reliable IR detectors. The work was performed in support of the Base and Installation Security System (BISS) program as a continuing effort to provide improved transducers for physical security sensors. The results of this work will be submitted to the BISSPO as a candidate effort for further pursuit in advanced development as a part of their overall imaging work.

Robert B. Curtis

ROBERT B. CURTIS
RADC Project Engineer

I.   INTRODUCTION

Intrusion detection and perimeter surveillance systems have been under development and applied by the military services for more than fifteen years. The earliest of these systems were passive line or point sensors utilizing conventional transducers (geophones, microphones, photoelectric devices, magnetic induction loops, pressure detectors, etc.) and simplified electronic designs. In general, these systems were developed for specific military field requirements and performed successfully under idealized or controlled application environments. However, false alarm disturbances experienced with these systems under more arbitrary and extreme environments indicated the need for continued development of improved sensors and detection system techniques. As a result of such continued development efforts, largely applied during the late 1960's and continuing to the present, more advanced intrusion detection systems evolved to take advantage of unique intrusion target signal signatures in more sophisticated signal processors to discriminate intrusion events from false alarms caused by localized natural environmental phenomena and cultural noise. These efforts led to the use of combinations of dissimilar target detection systems brought together with logic alarm decision circuits to identify intrusion signals. This type of signal analysis is an effective means of reducing false alarms. The more recent development efforts have been aimed at refining the target detecting transducers and developing new and improved transducer technology for intrusion monitoring applications.

To a very large extent, the investigation and development of advanced transducer technology for security systems has been fostered by the Base and Installation Security Systems (BISS) Tri-Service Program under the primary cognizance of the U.S. Air Force. These efforts have included surveys of fundamental transducer phenomena and physical processes, merit analyses of transducer mechanisms, selection of new transducer concepts, exploratory device research, and feasibility analyses of promising transducer techniques. The objectives of the research reported here were to provide an extension of the foregoing study efforts and was aimed at:

- °   The development of practical intrusion detection operational concepts and applications based on the pyroelectric and piezoelectric properties of polyvinylidene flouride film.

- °   The updating of the state-of-the-art survey of transducer mechanisms, materials, and devices as encompassed by previous efforts. The results of this survey are being published under separate cover.

Security systems for military bases and government assets have been selectively applied in several forms with success under BISS program guidance. The present state-of-the-art limitations in technical

1

system performance and implementation costs still present obstacles
to be overcome in providing more efficient and reliable intrusion
monitoring capabilities, in extending such coverage to a larger diversity
of assets, and in expanding the number and types of bases and installa-
tions protected. These limitations have led to the philosophy and
current BISS program emphasis of applying present-day intrusion detection
systems in the most practical and cost-effective applications possible,
namely, in protecting high value assets, and in undertaking exploratory
and advanced development programs which will ultimately yield more cost-
effective systems for wider spread use. The transducer development
studies and operational concepts which are reported here were directed
towards the BISS program emphasis and plan.

II.   TECHNICAL DISCUSSION

Previous studies of transducer mechanisms, materials and devices for intrusion detection applications[1,2,3] have identified and evaluated a number of potential transducer concepts for possible use in advanced security systems. The relative merits of these various techniques were established on the basis of their suitability for appropriate security monitoring applications, sensitivity to targets, operational limitations, potential problems, size and cost. The most promising techniques were selected for detailed investigation and/or experimental testing. From this work, the most successful results have been obtained with the pyroelectric polymer film Polyvinylidene Flouride (PVF_2) as a long wavelength room temperature infrared detector. PVF_2 film also has a piezoelectric sensitivity and as such has potential as an acoustic detector. In this regard, the pyroelectric and piezoelectric sensitivities of the polymer film make possible its use as a multi-mode, multi-purpose device. This section will discuss the general theory of pyroelectric and piezoelectric detectors.

A.   Pyroelectric Detectors

A limiting factor in the usefulness of any pyroelectric sensor is its signal-to-noise ratio. A commonly used expression of signal-to-noise ratio for a pyroelectric detector is its noise equivalent power

$$NEP = \frac{W}{S/N} \tag{1}$$

where W is the quantity of incident power required to produce a unity signal-to-noise ratio. If A is the active area of the detector and H the irradiance, W may be written as

$$W \simeq HA \tag{2}$$

Substituting this relationship into equation (1) gives

$$NEP = \frac{HA}{S/N} \tag{3}$$

It can be seen from equation (3) that the NEP is a function of the signal amplifier bandwidth as well as the detector area. To account for these two effects the NEP may be normalized by dividing by the square root of the product of the detector area and the bandwidth, Δf, of the signal amplifier. The reciprocal of the expression is designated as the normalized detectivity D^* [4]. That is,

$$D^* = (A \Delta f)^{1/2}/NEP$$
$$= (S/N) \left[(A \Delta f)^{1/2}/W \right] \tag{4}$$

3

The dependence of D^* upon the characteristics of the thin film detector configuration will be derived in the discussion which follows.

The defining equation for the pyroelectric effect is

$$\Delta P = p\Delta T \tag{5}$$

where ΔP is the change in surface charge density produced by a temperature charge ΔT. The proportionality constant p is defined as the pyroelectric coefficient. The total change in surface charge ΔQ is the product of ΔP and the transducer surface area A. The net current flow through the transducer is the time rate of change of the total surface charge, i.e.,

$$I = \frac{d}{dt} (\Delta Q)$$

$$= Ap \frac{d}{dt} (\Delta T) \tag{6}$$

In addition, the heat flow into the transducer element and the rate of heat energy storage within the transducer element are related to the quantity of absorbed energy by a statement of conservation of energy:

$$C \frac{d}{dt} (\Delta T) + G\Delta T = \eta HA \tag{7}$$

where:

C = thermal mass of the transducer;
G = thermal conductance of the transducer;
A = area of the transducer;
H = power density of incident radiation energy; and
η = efficiency with which the incident energy is absorbed

Any form of time variation may be analyzed by performing a Fourier transformation on each relation involved and examining the equations as functions of frequency. The corresponding amplitudes of each variable are represented as phasors, and the variation $e^{j\omega t}$ is always assumed but not expressed. Equations (6) and (7) are transformed into

$$\overline{I}(\omega) = j\omega p \; \overline{\Delta T}(\omega) \tag{7}$$

and

$$j\omega C\overline{\Delta T}(\omega) + G\overline{\Delta T}(\omega) = \eta \overline{H}(\omega)A, \tag{8}$$

where the barred symbols denote complex quantities. Equation (8) may be factored and solved for the quantity $\overline{\Delta T}(\omega)$

4

$$\overline{\Delta T}(\omega) = \frac{\eta \overline{H}(\omega)A}{G + j\omega C}$$

$$= \left(\frac{\eta}{G}\right)\left[\frac{\overline{H}(\omega)A}{1 + j\omega C/G}\right] \tag{9}$$

For the case where the excitation frequency is much higher than the thermal relaxation rate, i.e., $\omega >> G/C$,

$$\overline{\Delta T}(\omega) \approx \frac{\eta}{j\omega C} \overline{H}(\omega)A. \tag{10}$$

Since the thermal mass, C, of the film configuration is

$$C = c\rho dA \tag{11}$$

where:

c = specific heat of the sensor;
ρ = density of the sensor; and
d = thickness of the sensor element,

then the temperature change in the film is

$$\Delta T(\omega) = \frac{\eta \overline{H}(\omega)}{j\omega c\rho d} \tag{12}$$

Equation (12) may be substituted into Equation (7) to obtain

$$\overline{I}(\omega) = \frac{p\eta \overline{H} \omega A}{c\rho d} \tag{13}$$

The voltage produced across the sensor element is the product of the sensor impedance and current flowing through it. That is,

$$\overline{V}(\omega) = \overline{I}(\omega)\overline{Z}(\omega)$$

$$= \frac{p\eta \overline{H}(\omega)A\overline{Z}(\omega)}{c\rho d} \tag{14}$$

The noise effective power (NEP) of a detector is defined as the incident power necessary to produce a signal-to-noise ratio of unity. Rewriting equation (3) to show the frequency dependence gives

$$NEP = \frac{|\overline{H}(\omega)|A}{|\overline{V}(\omega)|/N(\omega)} \tag{15}$$

5

in which the Johnson noise voltage N( ), of the device is

$$N(\omega) = [4kT \; f |Z(\omega)|^2 / R]^{1/2} \qquad (16)$$

where:

k = Boltzmann's constant;
T = operating temperature in degrees Kelvin;
Δf = effective noise bandwidth of the associated amplifier; and
R = series equivalent resistance of the sensor.

Therefore, combining Equations (14) through (16), the noise effective power of the device becomes

$$NEP = \left[\frac{4kT\Delta f}{R} \right]^{1/2} \times \left[\frac{c\rho d}{p\eta} \right] \qquad (17)$$

The series equivalent resistance, R, of the transducer is

$$R = \frac{1}{\sigma A / d}$$

$$= \frac{d/A}{\omega \varepsilon \tan \delta} \qquad (18)$$

where:

σ = conductivity of the sensor element;
ε = dielectric constant of the sensor elements; and
$\tan \delta = \dfrac{\sigma}{\omega \varepsilon}$ = loss tangent of the sensor element.

Combining Equations (17) and (18) yields the final form

$$NEP = \frac{c\rho}{p\eta} (4KTA\Delta f d\omega \varepsilon \tan \delta)^{1/2} \qquad (19)$$

To account for the effects of noise contribution from the transducer area and the noise equilvalent bandwidth of the associated amplifier, a normalized detectivity (see equation 4) is defined as

$$D^* = (A\Delta f)^{1/2} / NEP$$

$$= \frac{p\eta}{c\rho} \left[\frac{1}{d\omega \varepsilon \tan} \right]^{1/2} \left[\frac{1}{4KT} \right]^{1/2} \qquad (20)$$

6

This formulation is based only on the assumption that the modulation frequency ω is much larger than the thermal relaxation frequency (assumed to be about 1 Hz by previous investigators).

All parameters except η, ω, k, T and ρ are influenced by the film type and the manufacturing process of the film. The conversion efficiency and modulation frequency parameters can be designed and optimized for a given application at the time of detector assembly design. Equation (20) also shows that D^* may be increased by decreasing the operating temperature of the device which for the transducers suggested in this work, is not very practical. The density of the film is an intrinsic parameter which cannot be controlled to any significant degree.

Other investigators have done PVF_2 parametric studies as suggested by equation (20). The data reported by Bergman et. al.[5] and Glass et. al.[6] demonstrates the pyroelectric coefficient, p, is inversely proportional to the film thickness. Consequently, very thin films of PVF_2 are desirable for maximum transducer detectivity.

Peterlin and Elwell[7] performed a series of measurements to determine the dielectric constant, ε, and the dielectric dissipation factor of rolled and unrolled PVF_2. The measurements were made as functions of temperature and frequency. The results demonstrated that the process of rolling PVF_2 produced a very significant change in the dielectric parameter dependence on temperature and frequency. Other studies have shown a dramatic decrease in the specific heat, c, of cold drawn samples of semicrystalline polymer samples [8]. The above expression for D^* indicates that a significant decrease in specific heat produces a correspondingly significant increase in normalized detectivity.

The thickness, d, of the PVF_2 film is the most directly controllable variable during manufacturing and post-manufacture processing. In addition to the explicit dependence on film thickness, as given in Equation (20), the thermal mass and hence the pyroelectric coefficient is seen to be inversely dependent upon the film thickness.

The absorption efficiency, η, is strongly influenced by the choice of material for the detector electrodes. The electrodes should be chosen for the highest possible absorption efficiency while maintaining ease and permanence of electrical attachment, and negligible electrode resistance (compared to the film resistance). The electrode on the incident face should be chosen to be absorptive and/or transparent for the wavelength range of interest and the transmissivity of the other electrodes should be minimized for the wavelength range of interest.

Equation (20) also indicates that the normalized detectivity is proportional to the reciprocal of the square root of the modulating

7

frequency, ω. The experimental measurements made by Phelan et. al.[4] demonstrate this frequency dependence. Consequently, the lowest modulation frequency consistent with the observation of moving targets is desirable.

In addition to the explicit dependence on temperature, the dielectric properties tanδ and ϵ are known to be functions of temperature[7], and the remaining material parameters are expected to also have a slight dependence on operating temperature. Since an increase in temperature leads to a deterioration of detectivity, and device cooling is assumed not to be feasible, the detectivity will be greatest whenever the heat generated by the associated electronics is isolated from the detector. This requires adequate thermal insulation between the electronics and the transducer surface, and requires design attention to provide adequate external heat sinking of the power dissipated within the electronics.

B. Piezoelectric Detectors

Many materials will display a charge on their surface after being mechanically manipulated or after exposure to an electric field or radiation. In general the charge will disappear after the cause is removed. In dielectrics, however, the material remains charged and as such is referred to as an electret.

Some electrets, of which PVF_2 is one, have the property of being both piezoelectric and pyroelectric. PVF_2 more specifically is referred to as a thermoelectret since it is sensitized by applying a high electric field at elevated temperatures. Electrets are commercially available as made from materials such as Mylar or Teflon. Nevertheless, the PVF_2 films show the largest piezoelectric effect known in polymers. The other characteristics which PVF_2 has which are not shared by the other materials are: (1) Elements with a large surface area and extremely thin cross section can be produced, (2) the film is highly flexible and light weight; and (3) it has an extremely large g-constant or stress constant.

The electromechanical constants commonly employed in characterizing the piezoelectric properties of the films are the strain constant d and stress constant g. For each of these, the directions of field, and stress or strain are indicated by two subscripts. The first subscript indicates the direction of the electric field and the second subscript indicates the direction of stress or strain.

The d constants express the ratio of strain developed along a specified axis to the field applied parallel to a specified axis, when all external stresses are constant. The d constants also express the ratio of short circuit charge per unit area of electrode which flows between connected electrodes which are perpendicular to a

8

specified axis, to the stress applied along a specified axis, when all other external stresses are constant. For example, if a frame of reference as shown in Figure 1 is used, then d_{31} denotes the ratio of
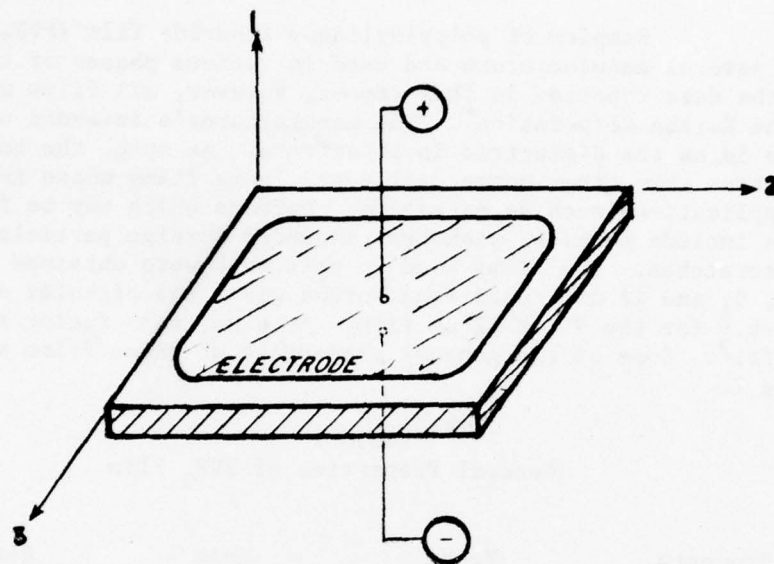

Figure 1. Reference Coordinates for
Piezoelectric Element

strain in the direction to the field applied in the 3 direction when the piezoelectric material is free in all directions. The coefficient d_{31} also denotes the ratio of charge per circuit area of electrode which flows between electrodes which are perpendicular to the 3 axis and connected together, to the stress applied in the 1 direction, when the material is free of external stresses in all other directions.

The g constants express the ratio of field developed along a specified axis to the stress applied along a specified axis when all other external stresses are constant. The g constants also express the ratio of strain developed along a specified axis to the electric charge per unit area of electrode applied to electrodes which are perpendicular to a specified axis. For example g_{33} denotes the ratio of field developed in the 3 direction to stress applied in the 3 direction when all other external stresses are zero. It also denotes the ratio of strain developed in the 3 directions to the charge per unit area of electrode applied to electrodes on faces perpendicular to the 3 axis.

9

III. RESULTS OF PVF$_2$ FILM STUDIES

A. <u>Pyroelectric Film Materials</u>

Samples of polyvinylidene flouride film (PVF$_2$) were obtained from several manufacturers and used in various phases of this work. For the data reported in this report, however, all films were supplied by the Kureha Corporation*. The manufacturer's intended use for these films is as the dielectric in capacitors. As such, the quality control is better than other commercially available films whose intended use is applications such as packaging. Defects which may be found in films include bubbles, pinholes, imbedded foreign particles, gouges and scratches. The films used in this work were obtained in thicknesses of 6, 9, and 12 μm. Data from Kureha gives the pinholes density as 0.1/ft.^{2} for the 9 and 12 μm film. At 6 μm, this factor increases to 0.5/ft.^{2}. Some of the general properties of these films are given in Table I.

Table I
General Properties of PVF$_2$ Film

Property	Value	Unit	Remarks
Density	1.8	gm/cm^3	
Water absorption	0.03	%	40°C, 90% RH
Melting point	180	°C	
Volume Resistivity	10^{15}	ohm cm	
Dielectric Constant	11.0		22°C, 60Hz
Dissipation Factor	0.012		22°C, 60Hz
Breakdown Voltage	6.5	KV (DC)	12 m film, 25°C

Polyvinylidene flouride film is chemically resistant to most inorganic acids, organic acids, alkaline materials, salts and oils at 25°C. A few organic solvents such as dioxane , acetone and monoethanolamine will react with the film in this temperature range.

The films were configured with metal electrodes, the choice of which will be discussed in a following section. Two mask assemblies were constructed for use in the vacuum depositions chamber.

_____

*Kreha Corporation of America
420 Lexington Avenue
New York, New York 10017

B.   Vacuum Deposition Techniques

The mask used in evaporating 2.5 cm (diameter) electrodes for the single-element-detector (SEL) is shown diassembled (after an evaporation) in Figure 2. The aluminum holder was designed for the fabrication of 4 elements on a single piece of film. The mechanical support for the mask was designed to allow it to be flipped 180° during the deposition procedure. Figure 3 shows the mask assembly mounted in the vacuum chamber as used for film preparation. Typical vacuum levels used were 5×10^{-5} mmHg or less. To prevent excessive heat from melting the film during the evaporation process, the filament was located 32 cm from the evaporation filament. With this type of holder and spacing, only metals with boiling points equal to or lower than aluminum could be evaporated without destroying the film.

The thickness of the evaporated film was monitored by a crystal detector placed in close proximity to the film. The crystal is an integral part of the digital measurement/display unit (Sloan Model DTM-200) which provides for in-process measurement of vacuum-deposited thin films. The thickness of the deposited films is calculated by measuring the change in period resulting from deposition of material on the sensor crystal. The signal processing unit computes and displays in Angstroms the equivalent film thickness with a resolution of 1 A° over the range used in this work.

The work represented here was, for the most part, directed towards the design, fabrication and testing of 2 different types of pyroelectric detectors. One type, the SEL has already been mentioned. A second design, the multi-element-detector (MEL) was directed towards the development of an infrared imager. For the MEL, a different holder was designed for the vacuum deposition of the film electrodes. For these detectors, an attempt was made to use nickel as the electrodes. Because of the higher boiling point of nickel, the holder was designed to provide for the heat sinking function and the evaporation filament was elevated above the film holder with a solid piece of aluminum on the under side of the film. A thin stainless steel mask was used to form the desired pattern on the surface of the film.

C.   Electrode Properties and Effects

The type of electrode to be applied to the PVF_2 film must be designed specifically for the application of the detector element. For a pyroelectric transducer, the IR properties of the electrodes must be designed to maximize the pyroelectric coefficient of the transducer. In prior pyroelectric work with PVF_2 films, various metals (4,6,9,10) such as nickel, aluminum and gold have been applied in thicknesses from a few tens to several thousand Angstroms. Electrodes for piezoelectric transducers of PVF_2 film require, on the other hand, more ruggedness and flexibility and less consideration for thermal properties.
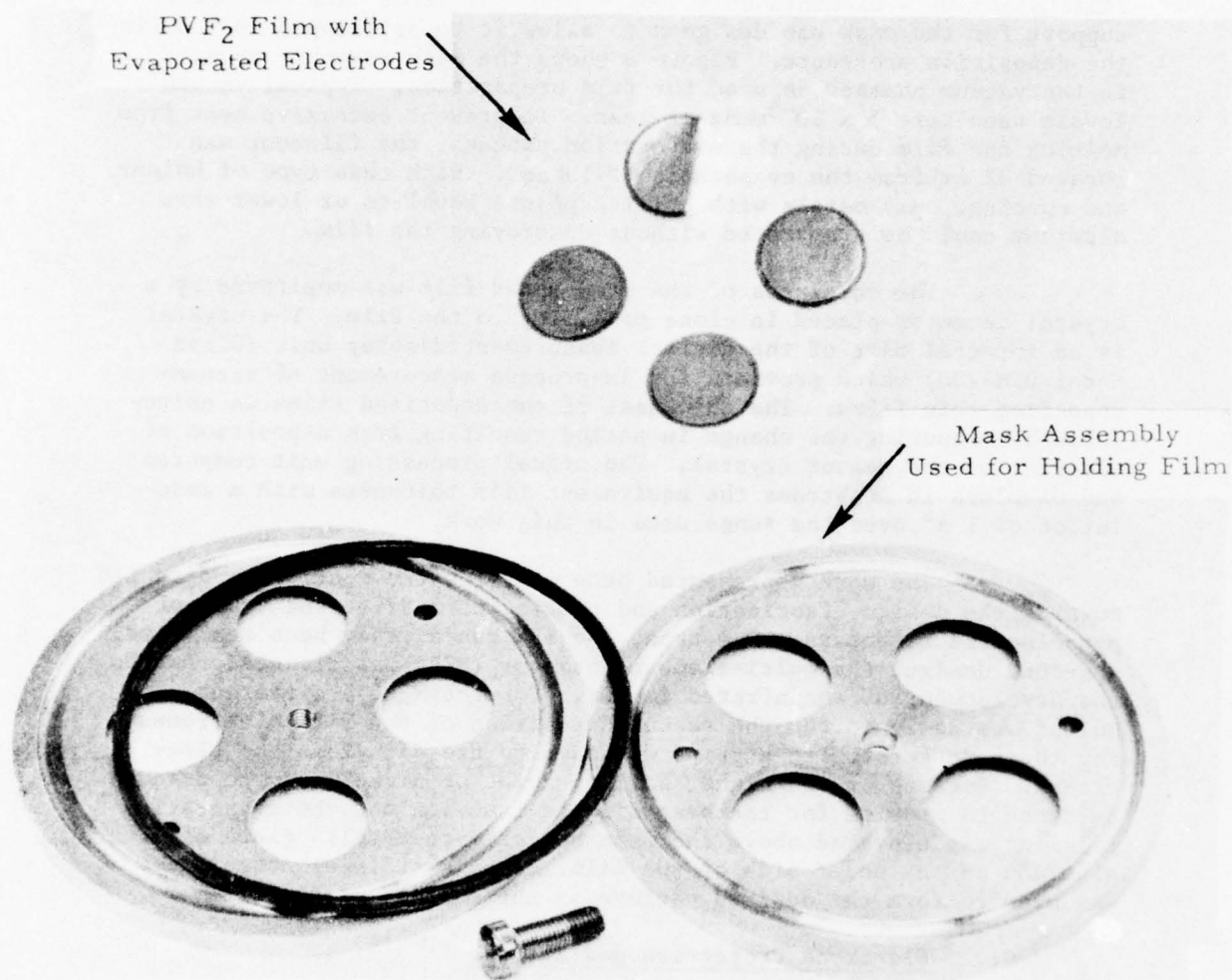
11

PVF$_2$ Film with
Evaporated Electrodes

Mask Assembly
Used for Holding Film

Figure 2. Mask Assembly and PVF$_2$ Film
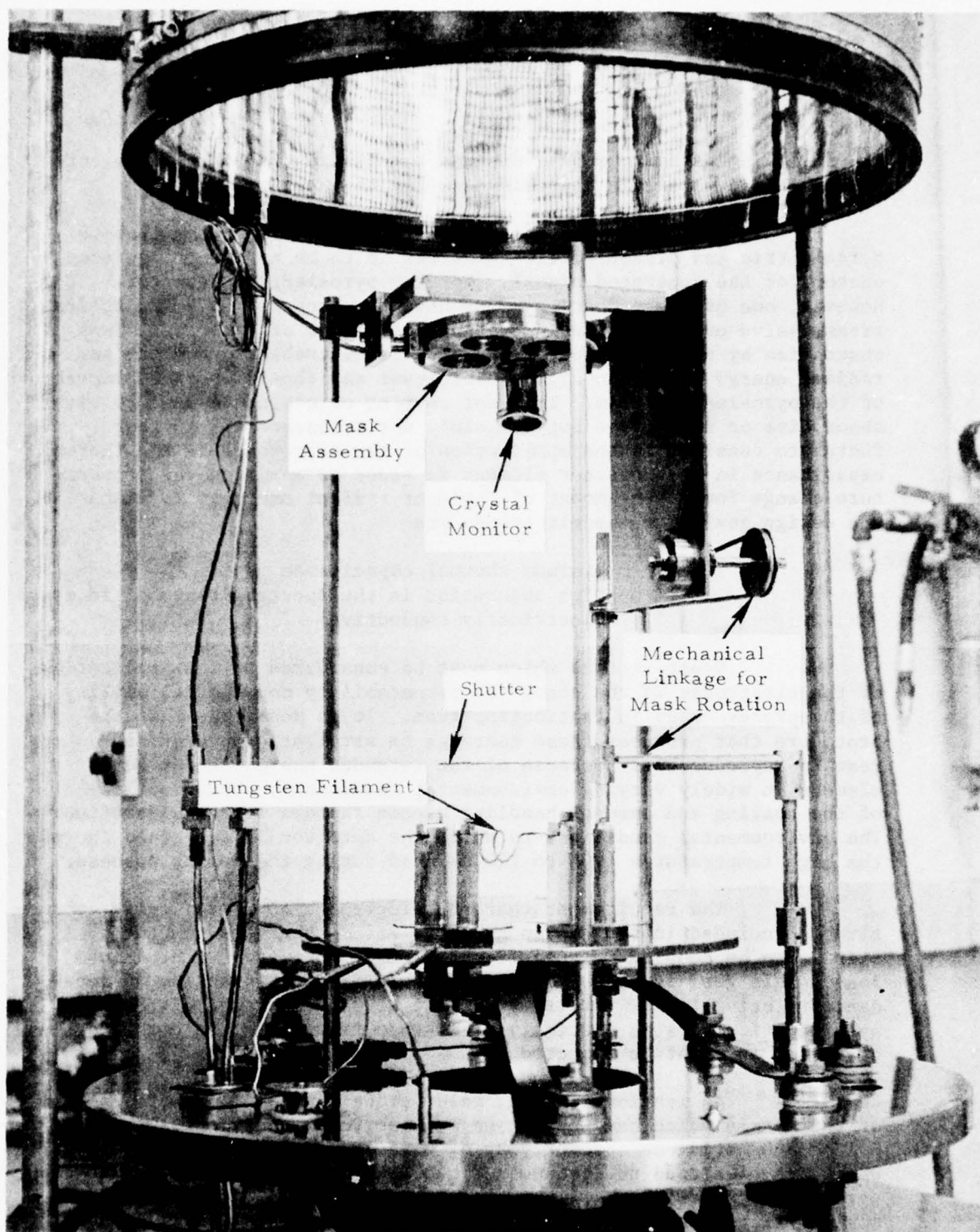Sample Shown Disassembled After Evaporation
of Electrodes

12

Figure 3. Vacuum Evaporation Chamber and
Film Evaporation Instrumentation

13

The following paragraphs will discuss the design tradeoffs in selecting electrode materials and thickness for the applications.

The primary purpose of the metallic electrodes in both pyroelectric and piezoelectric detectors is to be an electrical conductor for the generated signal. For the pyroelectric detector, however, one of these coatings must have the property of being optically transmissive or conductive in the spectral range of interest. This absorption by the electrode or the film is desirable to convert the radiant energy (i.e. the signal) into heat and thus raise the temperature of the pyroelectric film. The rear coating or electrode must be either absorptive or reflective but certainly not transparent. Another factor to consider in the application of the electrodes is the thermal capacitance in the detector element in order to maximize the temperature change for given amount of incident radiant energy. To summarize, the design goals for the electrodes are

- Minimum thermal capacitance
- High absorption in the spectral range of interest
- Electrically conductive

Other factors which must be considered in the application of the electrodes is the cost, the repeatability and the reliability of the process used in fabricating them. It is desirable that the procedure that produces these coatings be straightforward and the results reproducible. Because of the intended use of the detector element in widely varying environmental conditions, the durability of the coating and ease of handling become factors for consideration. The environmental conditions to which the detector is subjected include the high temperatures (90° to 110°C) used during the poling process.

The requirement that the electrodes be electrically conductive is included in the design goals to insure that the generated signal can be coupled to signal conditioning circuitry with minimum loss. This goal is met by designing the electrode to be low in impedance relative to the source. Since the source impedance of the pyroelectric films is extremely high, this requirement is not as stringent as might be expected.

As mentioned above, gold, nickel and aluminum are some of the metals which have been used as electrodes on PVF_2 films. Gold black having an absorptivity of 0.95 or greater is the most desirable electrode to achieve maximum sensitivity in an infrared pyroelectric detector. Of the choices available, it is also the most difficult to fabricate and the most fragile. For these reasons, no attempt was made to use gold black in this work.

14

If the film element is opaque over the optical wavelengths of interest, then the absorption of the signal does not necessarily need to occur in the electrodes. As will be shown, PVF_2 films do have a high degree of absorbance in the regions of interest. Thus, it is possible to use front side electrodes on the detector which are good electrical conductors but not ideal absorbers of radiation. Nickel is one of the metals which falls into this category with an absorption coefficient of 0.6 to 0.7 in the spectral band of interest. By making the coating thin enough, it will be only partially reflective and a large percentage of the incident radiation will therefore be either absorbed in the electrode or transmitted to the film to be absorbed, resulting in a detector whose efficiency is close to that obtainable by using gold black. Aluminum electrodes are another choice giving a performance approaching that of nickel. Because of the lower evaporation temperatures and the corresponding decrease in equipment complexity for the evaporation of electrodes, the majority of the detectors fabricated for this work were configured with aluminum on both sides. The front side electrode was typically 100 A° in thickness with the back side approximately 1000 A°. The thicker backplane electrode is necessary for mirroring the infrared radiation not absorbed by the film. This mirroring action results in a multiple transmission through the detector element with a corresponding increased absorption efficiency.

The peak spectral radiant emittance of a black-body source at 310°K (the temperature of the human body) occurs at the wavelength of approximately 10 µm. For sources at temperatures above that of the human body, the peak shifts to shorter wavelengths. Figure 4 shows a log-log plot of Plank's equation giving radiant emittance as a function of wavelength for black-body temperatures of 300°K (80.6°F) and 373°K (212°F). The peak emittance for these two curves varies from a wavelength of 7.8 µm for the 373°K curve to 9.7 µm for the 300°K curve. When Plank's equation is plotted on log-log coordinates, the shape of the black body curve is identical for all temperatures and for different temperatures need only be shifted along the line representing the Wien displacement law. This data is useful in evaluating the absorption characteristics of the electrodes and that of the PVF_2 film.

The IR absorbance spectra from 4 to 40 µm on a 9 µm sample of Kureha type KF PVF_2 film is shown in Figure 5(a). The measurement was made down to 2.5 µm but showed little variation from that shown between 4 and 6 µm. A significant amount of the radiant emittance of sources of interest (as shown in Figure 4) in intrusion applications, falls in the region of 7 to 10 µm where the film has high absorption peaks (i.e., low transmission).
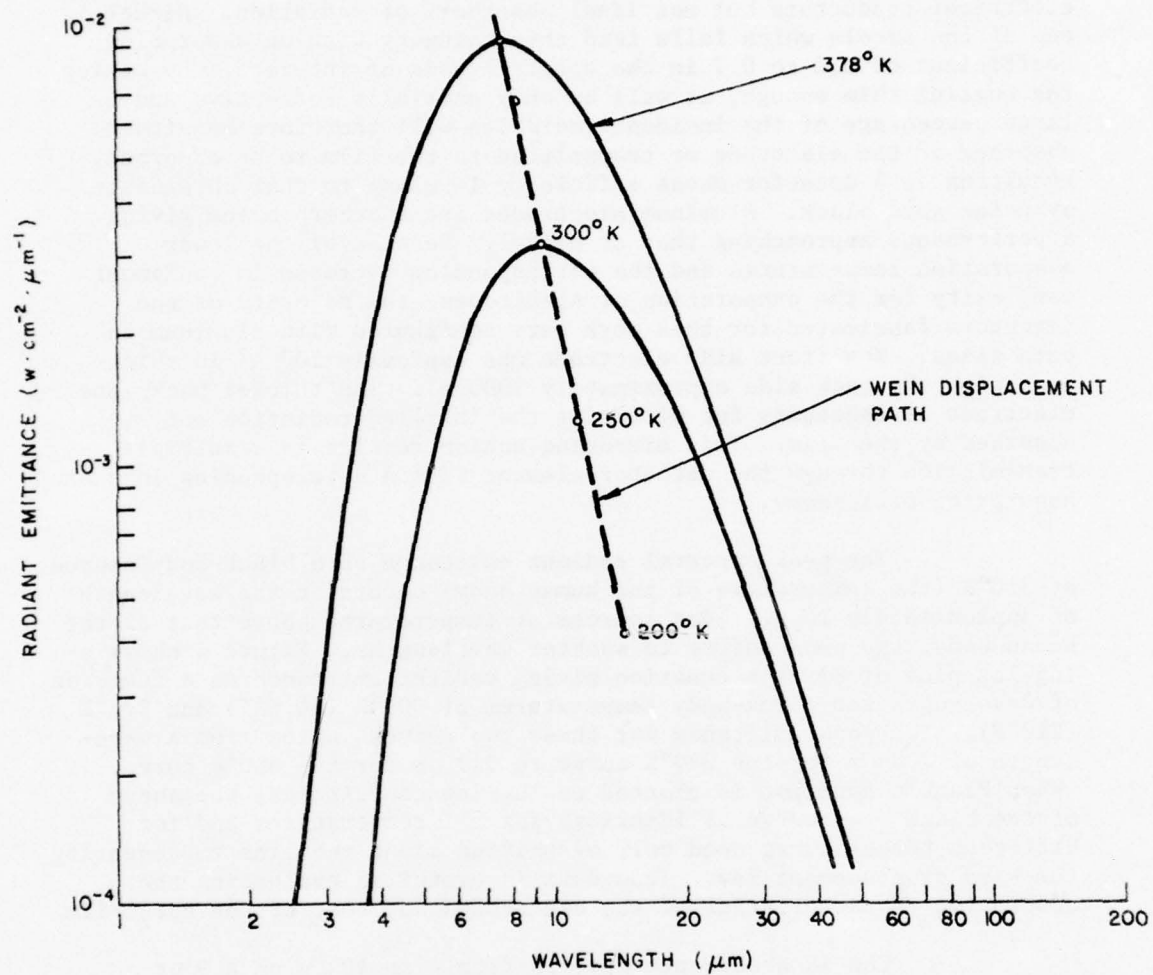
15

Figure 4. Radiant Emittance as a Function of
Wavelength for Black Body Temperatures of
300° K (81°F) and 373°K (212°F)

16

Figure 5. Infrared Absorbance Curves for (a) an Uncoated Sample of $9\mu m$ PVF$_2$ Film and (b) a $9\mu m$ Sample with 100A° Aluminum on One Surface
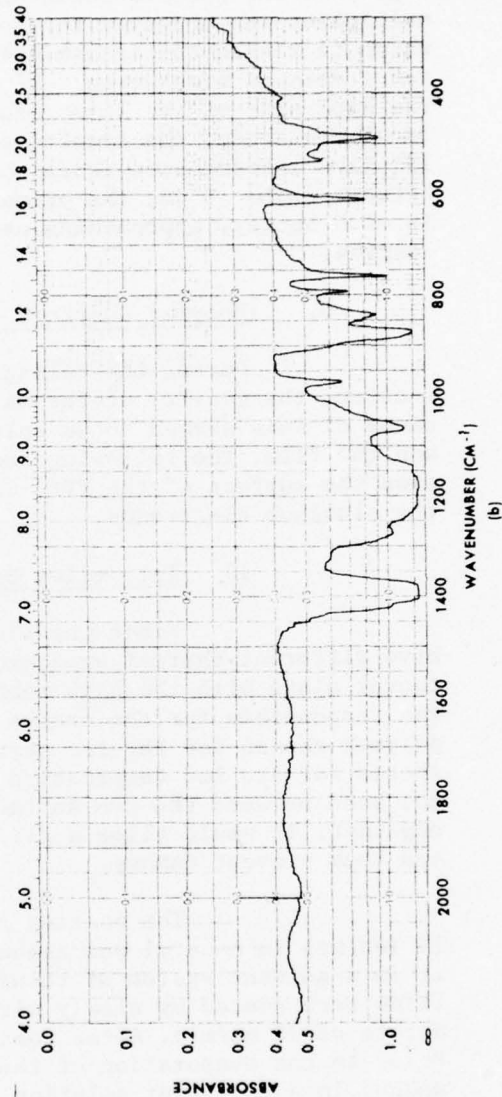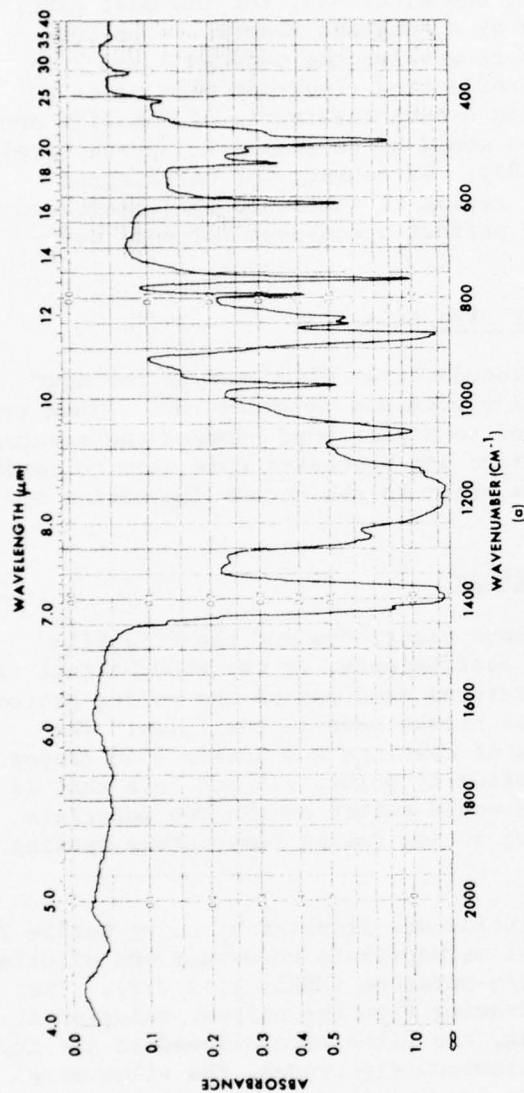

17

Figure 5(b) is the absorption spectra of a similar piece of 9 μm film coated with 100A° of aluminum on one side only. Comparing the two spectra curves it can be seen that the addition of the aluminum electrode results in an increased absorbance. For the region of the spectra shown here, the electrode, for the most part, multiplies the uncoated response by a constant absorbance factor which decreases the transmission at wavelengths between 4 and 7 μm for a one-way transverse. If a reflecting electrode were added to the back side of the film, causing a dual transverse of the film and front electrode, the transmission would be decreased to approximately 15% (i.e., absorbance equal to .82). Of course, for wavelengths between 7 and 10 μm, the primary region of interest, the absorption is much better, approaching near perfect opaqueness for some wavelengths.

D.   Polymer Coatings for PVF_2 Film

During the poling procedure, as discussed in the next section, the quality of the metal electrodes deteriorated. Since the cause of this seemed to be related to a poor bond between the electrode and the film, the following coatings and processes were used to condition the surface of the PVF_2 film prior to the vacuum deposition of the aluminum electrodes.

1)   1st Series Coatings

Since the aluminum electrodes and the PVF_2 film have different thermal expansion coefficients, it was thought that this factor along with the high temperatures used during the poling procedure was responsible for the cracks and breaks seen in the films. The polymer chosen for the 1st series of coatings was Lucite 2046 (Dupont) chosen for its low temperature softening point. It was felt that if the bond between the two surfaces would soften as the two materials expanded, it would allow a sliding action during temperature cycling and thus prevent damage.

The coating solution was prepared by using Lucite 2046, 1% (wt/wt) in n-butyl and isobutyl methacrylate copolymer and diluting it in a solvent system of toluene/q-butanone (MEK), (1:1 V:V). The films were coated by slowly withdrawing from the polymer solution at a rate of 20 mm/min. After coating, the films were allowed to air dry. Prior to the evaporation of the aluminum electrodes, the films were washed in a detergent solution (no scrubbing) and then rinsed in deionized water. Whereas the 100A° film deposited in one evaporation, the 1000A° side took two.

18

2)   2nd Series Coatings

For this series of coatings, the PVF_2 films were coated by withdrawing them from a 1% wt. solution of resin (2 parts by wt. of Shell's Epon (R) 828 and 1 part Ajicure B-002) in toluene-methyl isobutyl ketone (1:1, V:V). These films were also coated by slowly withdrawing from the solution at a rate of 22 mm/min. The coated films were allowed to air dry. Approximately one week elapsed between the coating of the films and the vacuum deposition of the electrodes.

E.   Poling Procedure

1)   Single Element Detector

Since the films of PVF_2 as received from the manufacturer are only slightly pyroelectric, to obtain a useable sensitivity they must undergo a poling procedure. This must be done after the electrode evaporation to prevent densitizing by the vacuum deposition process. The following steps outline the general procedure used in poling the elements. (1) The device was placed in an oven, (2) the oven temperature was elevated to the 90°C – 100°C range, (3) a poling voltage was applied across the electrodes for a specified period of time, and (4) the device was cooled to ambient while maintaining the poling voltage on the electrodes. Since a number of variations on this general procedure were tried, more details concerning those that led to both successes and failures will be given. At the outset of this study, the information available on the evaporation of the electrodes and the subsequent poling of the films was not available for successful fabrication of the detectors. A considerable amount of time during the project was devoted towards the development of these procedures.

In work done by Day, et. al.,[11] the poling conditions for PVF_2 detectors were investigated by fabricating a considerable number of detectors poled under a variety of conditions of temperature, voltage, and time. Their results showed that the responsivity of the pyroelectric detectors increases steadily with both voltage and temperature. Using 6 µm film with nickel electrodes, they found that the achievable responsivity is only limited by the ability of the film to withstand the high poling voltages and temperatures during the procedure. Although substantial scatter existed in data taken to test uniformity, the trends that are presented establish the fact that increased temperature and voltage also increase the uniformity as does increasing the poling time.

In the poling procedures, the two main causes of failure were: (1) the inability to maintain a good electrode and (2) the high voltage breakdown sometimes referred to as punch-through.

19

From an analysis of the films that failed during the poling process, it appeared that the primary contributing factor to the problems were the defects in the films alluded to earlier. In the case of losing continuity on the electrodes, the scratches, gouges and imbedded foreign particles created a discontinuity in the surface of the film which broke with the unavoidable flexing on the expansion/contraction phase which occurs during the temperature cycling used in the poling process. Figure 6 shows an example of film and electrode defects as observed under a microscope. The dark stripe across the field of view is a portion of one of the $100A^\circ$ aluminum electrodes used in the multielement detector. The near verticle break as seen in the photograph caused a loss of continuity in this electrode.

The high voltage breakdown points occur at the defect points mentioned above as well as the sites of pinholes or bubbles in the film. When punch-through occurs, a conductive path is established from one poling electrode to the other through the film. The extent of the damage is dependent upon the quality of the bond between the electrode and the film, the poling voltage and the size of the electrode being poled. As the arcing across the film starts in the region of one of these defects the heating apparently erodes away the film which further reduces the conductivity and helps sustain the arcing. In some cases the arc burned clean to allow a successful poling of the device; however, in the majority of the elements where this occurred, the failure was catastrophic. The probability of a high-voltage breakdown is dependent upon the quality of the film and the poling voltage and temperature.
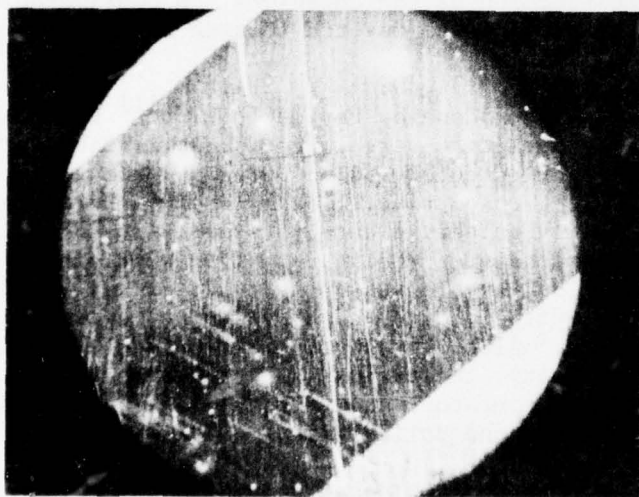

Figure 6. Magnified View of PVF_2 Film and Electrode Defects

20

A block diagram of the apparatus used for poling
the elements is shown in Figure 7. The output of the power supply
is coupled to the elements being poled through a large series resis-
tance (4 Meg ohms). This current limiting resistor is added to
limit the punch-through damage by limiting the maximum current available
if an arc occurs. Normally a negligible amount of current flows
because of the high impedance property of a quality detector element.
Nevertheless, the capacity of the element being poled contains a stored
charge which may be of significant magnitude for a large area element.
If, for instance, a detector element of 0.001 mfd capacity is poled
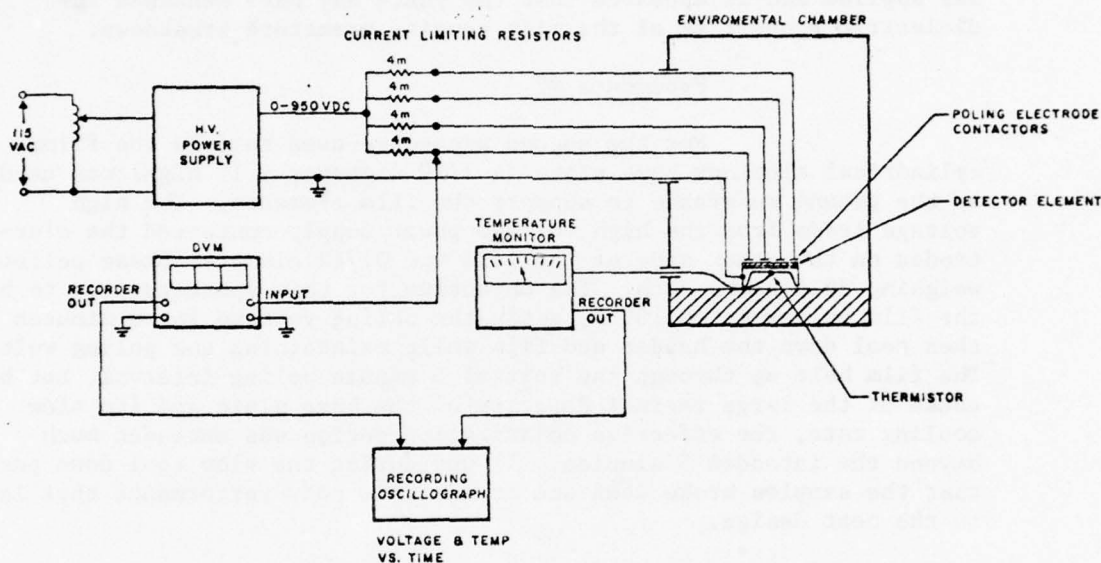at a voltage of 1000 volts, the stored charge would be 1×10^{-6} coulombs.

Figure 7. Apparatus Used for Poling the PVF_2 Detector Elements

If this charge is dumped in 1×10^{-6} seconds, at the onset of an arc,
a current of 1 amp would be established during the discharge. This
type of discharge negates the protection provided by the series limiting
resistors on the output of the power supply.

In attempting to fabricate quality detectors, a
number of poling techniques were tried. In some cases the film/elec-
trode element was poled and then mounted into a mechanical support;
in other procedures the element was first mounted and then poled. A
brief discussion of the techniques is given in the sections which follow.

21

Procedure #1

In the first poling procedure attempted for this work, the 1-inch diameter single-element-detector (SED) was mounted on the copper clad fiber glass rings which was designed to be used in the holder for the detector. The element fabricated from 12 μm Kureha film was stretched across and fastened to the ring using a silver paste* epoxy type compound. Each attempt to pole the film in this manner resulted in a voltage breakdown which occurred from 300 vdc to 500 vdc. Examination of the element under a microscope revealed that the punch-through occurred near the points where the silver paste was applied and it appeared that the paste may have weakened the dielectric properties of the film causing premature breakdown.

Procedure #2

For the second procedure used to pole the films, a cylindrical aluminum base plate (4-1/2" diameter x 1" high) was used as the ground reference to support the film elements. The high voltage leads from the high voltage power supply contacted the electrodes on the other side of the film via 0.712 diameter brass pellets, weighing 20.5 grams each. The objective for this apparatus was to bring the film holder up to 100°C, apply the poling voltage for 5 minutes and then cool down the holder and film while maintaining the poling voltage. The film held up through the initial 5 minute poling interval, but because of the large thermal capacity of the base plate and its slow cooling rate, the effective polarization period was extended much beyond the intended 5 minutes. It was during the slow cool down period that the samples broke down and it was this poor performance that led to the next design.

Procedure #3

The apparatus used in this procedure was similar to that described in #2 with the exception of the base plate used for the ground electrode. The supporting element as sketched in Figure 7 was cut from an aluminum cooling extrusion (Wakefield Engineering, Inc., No. 1527) normally used as semiconductor heat sinks. The plate side of the base element was polished to provide a smooth surface for contacting the film electrodes. The finned underside was painted flat black to increase the emissivity and the cooling rate. The format for poling the films using this apparatus is as follows:

---

*Eccoband solder 56C, Emerson & Cumming, Inc., Canton, Mass.

- The detector elements as received from the vacuum deposition chamber are placed on the finned aluminum heat rink.

- The brass weights with current limited high voltage leads attached are placed on the top side of the detector elements.

- The chamber and holders are warmed to 100°C.

- The high voltage is slowly applied.

- When the poling voltage is reached, the voltage and temperature are maintained for 5 to 10 minutes.

- At the end of the poling interval, the chamber and holder are cooled to ambient temperature while maintaining the poling voltage. This cooling interval typically took 10 to 15 minutes.

- The detector elements are cut from the mother sheet and mounted on the ring holders for subsequent testing.

This technique was the most successful in poling the SED elements but it, as well as the others, still depends on the quality of the pyroelectric material for success.

Procedure #4

Another approach tried (not in chronological order with those listed above) in an attempt to increase the yield during the poling procedure utilized the detector holder as described later in Section III-F. To prepare for this procedure, the film was mounted using the hardware fabricated for the holder. The detector elements which were poled in this manner suffered a high voltage punch-through at about 1/3 to 1/2 the attempted final value. An examination of the elements after removal from the holder revealed that the perimeters of the film, where the contact pressure had been applied, apparently had had a great deal of pressure applied. A calculation of the thermal expansion of a Deldrin sleeve used in the holder showed that its expansion at the elevated poling temperatures would account for the pressure effects seen. Because of the success of the procedure #3 as discussed above, the in-holder poling procedure was not pursued further.

23

2) Multielement Detectors

The poling procedure described above, which worked for the single element detectors, was inadequate for use with the multi-element detector used in the infrared imager. In the single element detector, a small break or blemish in the coating was inconsequential because of the circular contacting ring around the element giving a full 360° of conduction paths. For the infrared imager, however, the element on one side of the film consists of a long and narrow strip with electrical contact made only at one end. Thus a small blemish across the electrode can cause a complete break in the metal resulting in a partial or sometimes complete severing of the sensitive area. What appeared to be a good element after vacuum deposition of the electrodes would be defective after the poling procedure.

To fabricate a usable detector then, 2 techniques needed to be improved; (1) a better quality electrode was needed on the film surface and (2) a different approach to the poling procedure was needed. Described in the sections which follow are the poling techniques which were used in evolving a usable method. The vacuum deposition and film preparation development are described elsewhere in the report.

Procedure #5

Subsequent to the design and construction of the evaporation mask for the MED (multi-element-detector) it was determined that stress points in the overlapping electrode regions could cause premature voltage breakdowns. For this reason, the masks used in the MED were designed with electrode areas on both sides of the film where no overlap occurred. Hence, to achieve a maximum poling field, the mounting hardware used was also designed with the electrical leads contacting the metal films on areas away from the overlapping region. This approach avoids sharp edges and strains in the high field regions that could cause voltage punch-through failures.

The first poling procedure tried was a modification of #3 discussed above. The MED was placed on the aluminum heat sink with the 1000 A° back plane down. To avoid stress points across the 100 A° strips on the top side, a strip of silver impregnated foam (designed for use as RFI gaskets) was laid across the connecting tops, away from the overlapping electrode region. After the poling procedure cool-down, it was found that the gasket material had bonded to the aluminum and peeled off the electrode as it was removed. Other contactors were tried in place of the conductive foam but all resulted in an intolerable amount of damage to the detector.

Procedure #6

Elements which appeared to be usable after poling as described in procedure #5, were found to be defective after mounting in the film holder. It was never ascertained whether the damage occurred during the poling process or as a result of the handling during mounting. Thus, the next and the most successful approach tried was to mount the film in the fiber glass holder before poling. The holder was designed to avoid pressure points in the areas of electrode overlap. This design serves a two-fold purpose; (1) the pressure stress points, and (2) dielectric weakening due to the silver epoxy paste is eliminated in the overlapping electrode regions of the film.

During this phase of testing a second silver paste was tried for assembly of the detector. This paste which uses a phenolic base is designed to be used for forming conductors in hybrid circuits. The paste, however, uses a heat cure and does not become conductive until cured. Since the curing temperature is above the melting point of PVF_2, this paste was deemed unusable for this application.

Procedure #6 worked well in preventing the high voltage punch through and minimized the electrode damage as caused by #5. Nevertheless, this procedure still resulted in a near zero yield because of discontinuities which developed in the 100 A° electrode strips. The polymer coatings which were tried to develop a better bond between the electrode and the film (see Section III-D) were worked on concurrently with the poling procedures and it was this joint effort which led to procedure #7.

Procedure #7

As mentioned above, the main failure mechanism seen in technique #6 was the loss of electrode material and the generation of discontinuities which occurred during the poling cycles. A distinct crazed surface developed on the films which had been dipped in the thermo-setting epoxy. Speculation on what was causing this phenomena led to the postulate that at high voltages and temperature, the thin aluminum film was oxidizing resulting in a brittle surface with a decreased tenacity. To overcome this problem, it was decided to back-fill the poling chamber with an inert gas before elevating the temperature of the film and applying the poling voltage. A vacuum type environmental chamber was used for this technique and the following scenario was followed during the process.

25

- The oven, requiring 4 hours for heating, was pre-heated to 100°C.

- The chamber was evacuated to a pressure level of approximately 50 mmHg and then back-filled with N_2 to atmospheric ($\approx$ 760 mmHg) pressure.

- The film holder was quickly inserted into the chamber to minimize the mixing of N_2 with room air.

- The vacuum pump was started again concurrently with the bleeding of N_2 into the chamber. The chamber was again evacuated down to 50 mmHg. The pump was turned off and N_2 was again used to bring the pressure to approximately 660 mmHg. At this point the film element had reached 100°C.

- The poling voltage was applied for 5 minutes.

- The chamber was brought back to atmospheric pressure using N_2 and the chamber was opened and the film holder was removed from the chamber.

- While still maintaining the poling voltage, the film was cooled to ambient temperature - then the voltage was removed.

This procedure did not help the crazing seen in the polymer coated film (Section III-D) which were prepared using the 1st series of coatings. Success was achieved, however, using the film specimens which had been coated using the 2nd series of coatings and procedure #7. A usable detector element was also obtained with an un-coated film and procedure #7. Due to the success obtained using this poling technique, then this was the best and final procedure used in this work.

     F.   Construction and Testing of the Single Element Detector

The technical discussion presented in Sections II.A and II.B give the rationale behind the fabrication of the sensing element used in the single element detector. Results of sensitivity tests made with the element and details on the construction of the detector and associated circuitry are given in this section.

    1)   Mechanical Holder

Figure 8 shows a picture of the SEL holder as used for housing the PVF_2 film for testing. The film after poling as
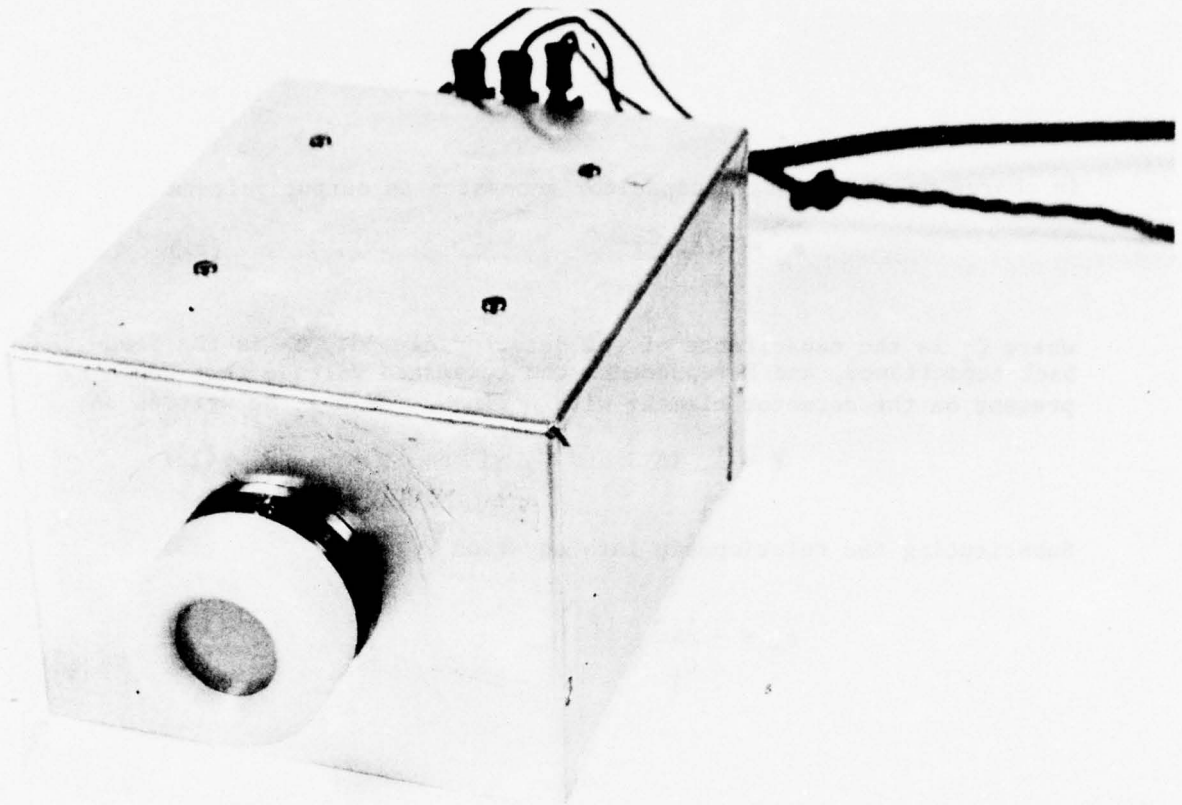
Figure 8. Single Element Detector (SEL) Holder and
Breadboard Container for Signal Conditioning Circuitry

described in Section III-E-1 was fastened to a fiberglass ring using
a conductive silver paste. This supporting structure was then placed
inside the cylindrical holder with a small copper ring on the front side
to make electrical contact with the frontside electrode on the film.
A Irtran II IR filter was placed in front of the film to protect the
film from acoustic vibration and thermal fluctuations which would   .
limit the ability to make pyroelectric sensitivity tests on the film.

2)   Figure 9 shows a schematic of the signal conditioning
circuits furnished with the single element detector (SED). The first
stage in the two-stage circuit consists of an operational amplifier
configured as a charge amplifier. The design equations and operational
characteristics will be described in the paragraphs which follow.

When the detector is connected to the inverting
input of an operational amplifier, configured as a charge amplifier,
the generated charge flows into the feedback capacitor. The change

27

in charge on the feedback capacitor generates an output voltage

$$e_o = -(\Delta E)\frac{C_1}{C_f}$$ (21)

where C_1 is the capacitance of the detector element, C_f is the feedback capacitance, and E represents the generated voltage that would be present on the detector element with no load. ΔE may be written as

$$E = \frac{1}{C_1}\ I\Delta T$$ (22)

Substituting the relationship into equation 21, (23)
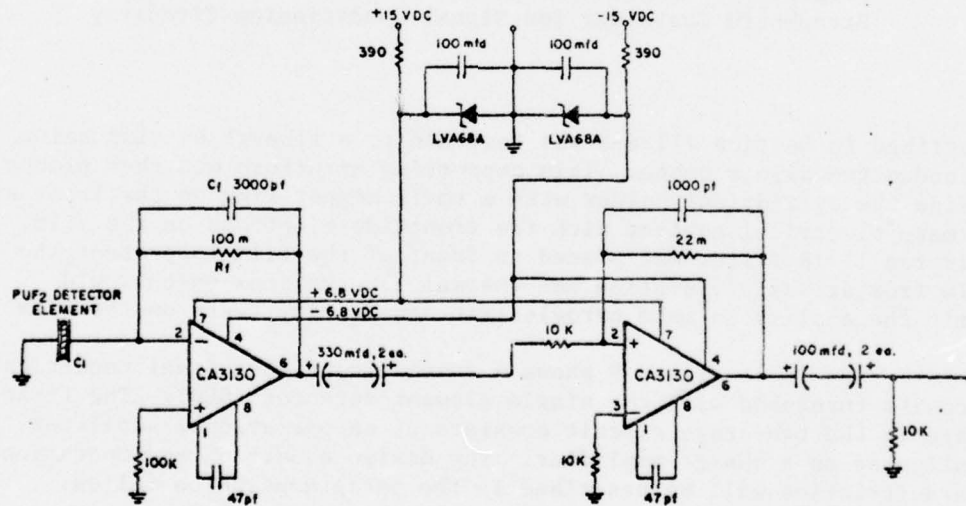
$$e_o = -\frac{I\Delta T}{C_f}$$

Figure 9. Single Element Detector Circuit

28

A typical value for I is 7.18×10^{-11} amps. Using this value for I, a ΔT of 1 second and a $C_f = 0.003$ mfd gives

$$e_o = - \frac{(7.18) \ (10^{-11}) \ (1)}{(.003) \ (10^{-6})} = 0.0239 \text{ volts}$$

To supply bias current to the inverting input of the charge amplifier, a feedback resistor R_f is added in parallel with the feedback capacitor C_f. This resistor limits the lower frequency response to $1/R_f C_f$ radians per second. For the values shown in the schematic ($C_f = 3000$ pf and $R_f = 100$ Megohms), the corner frequency occurs at 3.33 rad/sec or 0.53 Hz.

For frequencies in the passband, the gain is set by the ratio of the detector capacitance C_1 to that of the feedback capacitance (C_f/C_f). As used here, the feedback capacitor was selected to make this ratio close to unity.

It is desirable to use a small value of C_f for maximum gain; however, this capacitor must be selected to be consistent with the desired low frequency response and a reasonable value for R_f. FET amplifiers are usually used in charge amplifiers because of their low bias current, and high input impedance.

The charge amplifier output is coupled to a post amplifier (U101) which supplies an additional gain of 67 dB to the detector generated signal. A feedback capacitor on this stage limits the upper frequency bandwidth to approximately 8 Hz. The output impedance of the amplifier is 10 K ohms set by the 0.3 Hz high pass network added to the output of the post amplifier. The amplifiers are powered by a $\pm$ 15 VDC supply.

Test Results

The noise equivalent power NEP and detectivity D^* were measured using a black-body with a mechanical chopper in front of the source. In the tests reported here, the temperature of the black-body ranged between 350°K and 450°K. The size of the chopping aperature was larger than the diameter of the black-body opening so the chopped radiation coming from the black-body was limited by its size. The detector was placed at a fixed distance from the source. This distance was selected to be approximately ten times the diameter of the black-body aperature.

The detector output voltage was measured using a PAR, model 124 lock-in amplifier. The demodulating signal was derived from

29

a sync signal generated by the rotation of the IR chopper wheel. The noise measurements were made by covering the exit part of the black-body. During these tests, the time constant switch on the lock-in amplifier was switched to a position giving an effective bandwidth of 1 Hz. The output of the amplifier was read on a self-contained rms voltmeter.

Using the measurements obtained under the experimental conditions described above, the characteristics of the pyroelectric detectors was measured. The equations and the step-by-step procedure used in calculating D^* is as follows:

(1) The emissive power of the black-body compensated for ambient conditions is calculated as:

$$W_o = \sigma(T^4 - T_o^4) \qquad \text{watts/cm}^2 \qquad (24)$$

where

$\sigma = 5.669 \times 10^{-12} \qquad \text{watts/cm}^2/{}^o_K{}^4$

T = absolute temperature of source ${}^o_K$

T_o = ambient temperature $\qquad {}^o_K$

(2) At some distance from the black-body, the irradiance H_o at the detector is:

$$H_o = \frac{W_o A_s}{\pi r^2} \qquad (25)$$

where

A_s = area of black-body port $\qquad \text{cm}^2$

r = distance to detector $\qquad \text{cm}$

(3) The noise equivalent power is calculated as:

$$NEP = \frac{H_o A_d}{V_s/V_n} \qquad (26)$$

where

A_d = area of detector $\qquad \text{cm}^2$

V_s = signal voltage $\qquad \text{rms volts}$

V_n = noise voltage $\qquad \text{rms volts}$

(4) The detectivity is then calculated as:

$$D^* = \frac{(A_d \Delta f)^{1/2}}{NEP} \qquad \text{cmHz}^{1/2}/\text{watt} \qquad (27)$$

where ΔF - bandwidth of the lock-in amplifier.

30

After compensation for the square wave nature of the chopped radiation, IR losses by the Irtran filter and frequency response corrections for the detector, the representative sample of values presented in Table II were calculated. Although other metals were tried for evaporating the electrodes, all results reported in Table II were for Kureha type F films with aluminum electrodes on both sides.

Table II
Test Results for Single Element PVF_2 Pyroelectric Detectors

Sample No.	D^* $cm(Hz)^{1/2}/watt$	Film Thickness (μm)	Poling Time (min.)	Poling Temp (°C)	Poling Field (volts/cm)
1	4.34×10^5	12	20	100	833
2	5.48×10^5	12	7	101	833
3	1.25×10^7	12	7	101	833
4	3.41×10^6	12	5	100	833

Discussion of the Results

The results shown in Table II are comparable to but no better than other pyroelectric detectors fabricated from PVF_2 films as reported in references (2) and (4). As this project progressed, awareness of recent work by other investigators with some of the same objectives was gained. For example, a thorough investigation of the factors involved in optimizing the poling procedure has been published by Day, et. al. [11] For these reasons, towards the close of the experimental phase, the objectives of the work were concentrated towards the development of intrusion detector concepts as opposed to the optimization of the pyroelectric effect. It is this device development which is reported in the next section.

G. Construction and Testing of Multiple Element Detector

New materials and recent advances in integrated circuit technology have provided the impetus for developing flat-panel image sensing and display devices. Such devices have the obvious advantage of replacing the electron beam tube which is generally used in conventional pick-up and display devices. With reference to intrusion detection devices, most infrared imaging detectors are effective for their intended purpose. Most are very expensive, however, and are not well suited as a cost effective device for protecting extended areas. The device developed here is designed to test the feasibility of applying the current technology of PVF_2 film towards the development of a low cost infrared imaging detector.

31

A small, low resolution prototype PVF$_2$ infrared imaging system which is described below has been built and operated successfully. Testing was performed by imaging infrared radiation at the rate of 16 frames per second.

1) Theory of Operation

An infrared intrusion detector may, in general, be used to detect humans or vehicles. Of the two types of signal sources, the human represents a worst case infrared target since the associated temperature will be lower than that of hot spots found on most vehicles. The following discussion will apply to the detection capabilities for human targets.

The thermal radiation over most of the human body is attenuated by clothing. The most consistently exposed portions of the body are the hands and the heads. For this discussion, then, the detection capabilities with reference to the head will be considered.

If the human head is approximated as a sphere 12 cm in diameter, then at a distance, this sphere will be seen as a disc of area

$$A_s = 113 \text{ cm}^2$$

$$= 0.0113 \text{ m}^2$$

Now for a black-body at 98.6°F (310°K) the radiant emittance is

$$W = \sigma T^4 \qquad \qquad (28)$$

$$= 0.0524 \text{ watts/cm}^2$$

where the Stefan-Boltzman constant $\sigma = 5.67 \times 10^{-12} \text{ W cm}^{-2} \text{ °K}^{-4}$.

If it is assumed that the emittance of the skin is $\varepsilon = 0.9$, then the radiant emittance for the head would be

$$W' = (0.9)(W)$$

$$= 0.047 \text{ watts/cm}^2$$

$$= 471 \text{ watts/m}^2$$

32

At a distance R from the sphere, the total radiant flux P incident on a detector with an aperture area, A_a, is

$$P = \frac{A_s\, A_a\, W'}{\pi\, R^2}$$

(29)

where A_s = area of the source

Now if a lens or spherical mirror with a diameter of 5.2 cm is used as a radiation gatherer, the aperture A_a is $(2.6)^2$ or 21.2 cm^2. If 50% of the mirror is blocked by hardware, the effective aperature is 10.6 cm^2 = 1.06 x 10^{-3} m^2. For R = 5 meters, W = 471 watts/m^2, and A_s = .0113 m^2, equation (29) gives

$$P = \frac{(.0113)(1.06 \times 10^{-3})\,(471)}{\pi\,(5)^2}$$

= 7.18 x 10^{-5} watts.

A typical D* for a quality pyroelectric PVF$_2$ detector is approximately 1 x 10^8 cm. Hz$^{1/2}$ W^{-1}. The current responsitivity for this same detector would be

$$R_I = 1 \times 10^{-6} \text{ Amp/watt}$$

Multiplying this factor by the radiated power incident upon the detector gives the total current into a short circuit as

$$
\begin{aligned}
I &= (R_I)(P) \\
&= (1 \times 10^{-6})(7.18)(10^{-5}) \\
&= 7.18 \times 10^{-11} \text{ amps}
\end{aligned}
$$

If the feedback capacitor in the charge amplifier is 0.001 mfd and the capacitor of the detector element is 0.0013 mfd, then the steady state gain of the charge amplifier is 0.001/.0013=0.77. If a human target as assumed above is in view for 1 second, then the total charge developed versus the charge amplifier feedback capacitor is

$$
\begin{aligned}
V &= I\,\frac{\Delta t}{C} \\
&= (7.18)(10^{-11})(1)/(.001 \text{ mfd}) \\
&= .0718 \text{ volts.}
\end{aligned}
$$

33

This signal with a little post amplification is of sufficient amplitude to drive a comparator stage for establishing a threshold to provide target discrimination. With these design equations, the hardware and circuits which are described in the next section were developed to test the feasibility of such a device.

(a) Sensor Construction

An exploded view of the IR imager detector is shown in Figure 10. The PVF_2 film element was assembled in this holder prior to poling as described in Section III-E-2. In this illustration for purposes of clarity, the 100 A° and 1000 A° vacuum deposited electrodes are shown as distinct elements which are separable from the PVF_2 film. The film was sandwiched between two end pieces fabricated from fiberglass material (glass reinforced PC board). A conducting copper strip on the front plane side was used to make electrical contact with the 100 A° electrode which is the semi-reflecting side used to absorb and transmit the incident radiaton. A single conductor tied to this electrode is returned to circuit common in the electronics described in the next section.
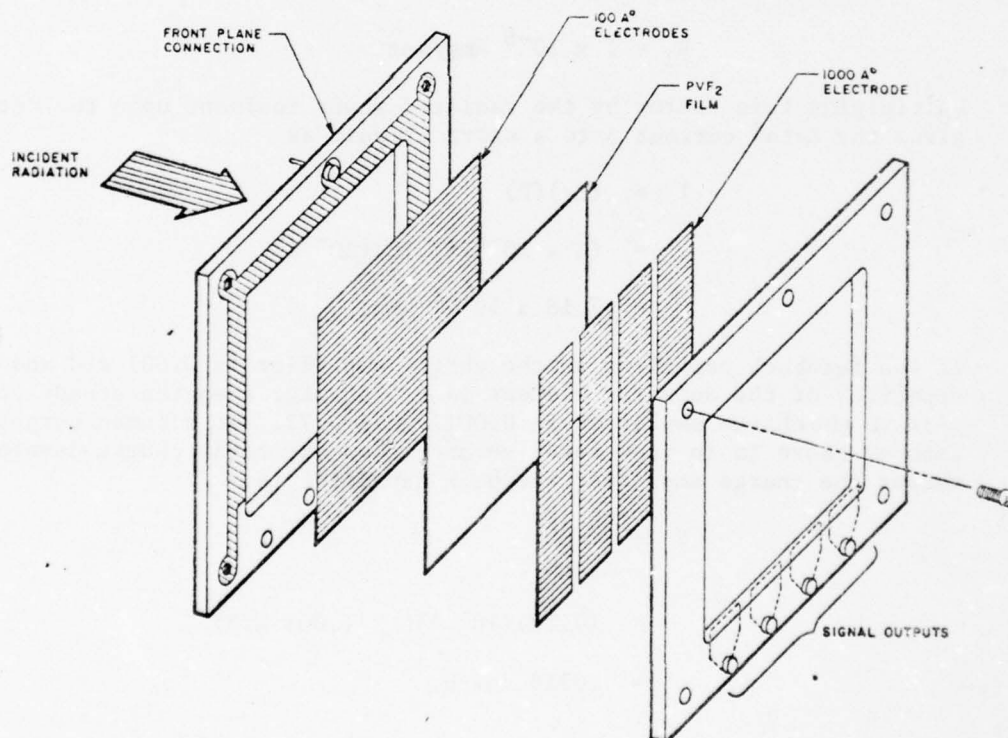

Figure 10. Exploded View of the Detector Element
Used in the Infrared Imager

The other fiberglass support element has 4 copper clad electrodes which make contact with the 1000 A° film electrodes shown in Figure 10. Signal output connector pins soldered to these conducting pieces are designed to plug into the charge amplifier module. A picture of the assembled detector is shown in Figure 11. Prior to poling, the film is stretched tight in the holder and secured with the 4 screws on the corners. Conductive silver paste was used for maintaining electrical continuity between the copper clad strips and the aluminum electrodes. The heating-cooling cycle which was used during the poling procedure causes the film to expand and contract and results in the wrinkled appearance which is apparent in the photograph.
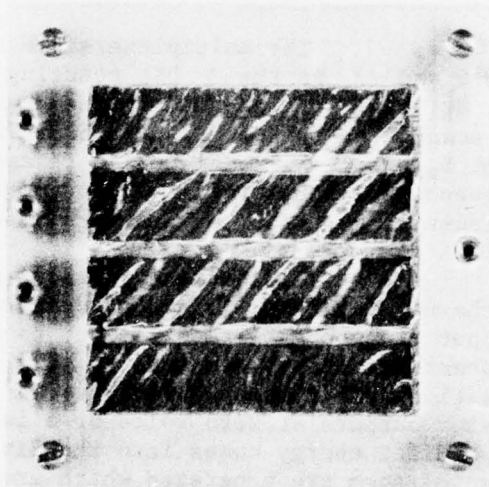

Figure 11.   Assembled Detector for Use in Infrared Imager

2.   Circuit Description and Construction Details

b. Circuit Description
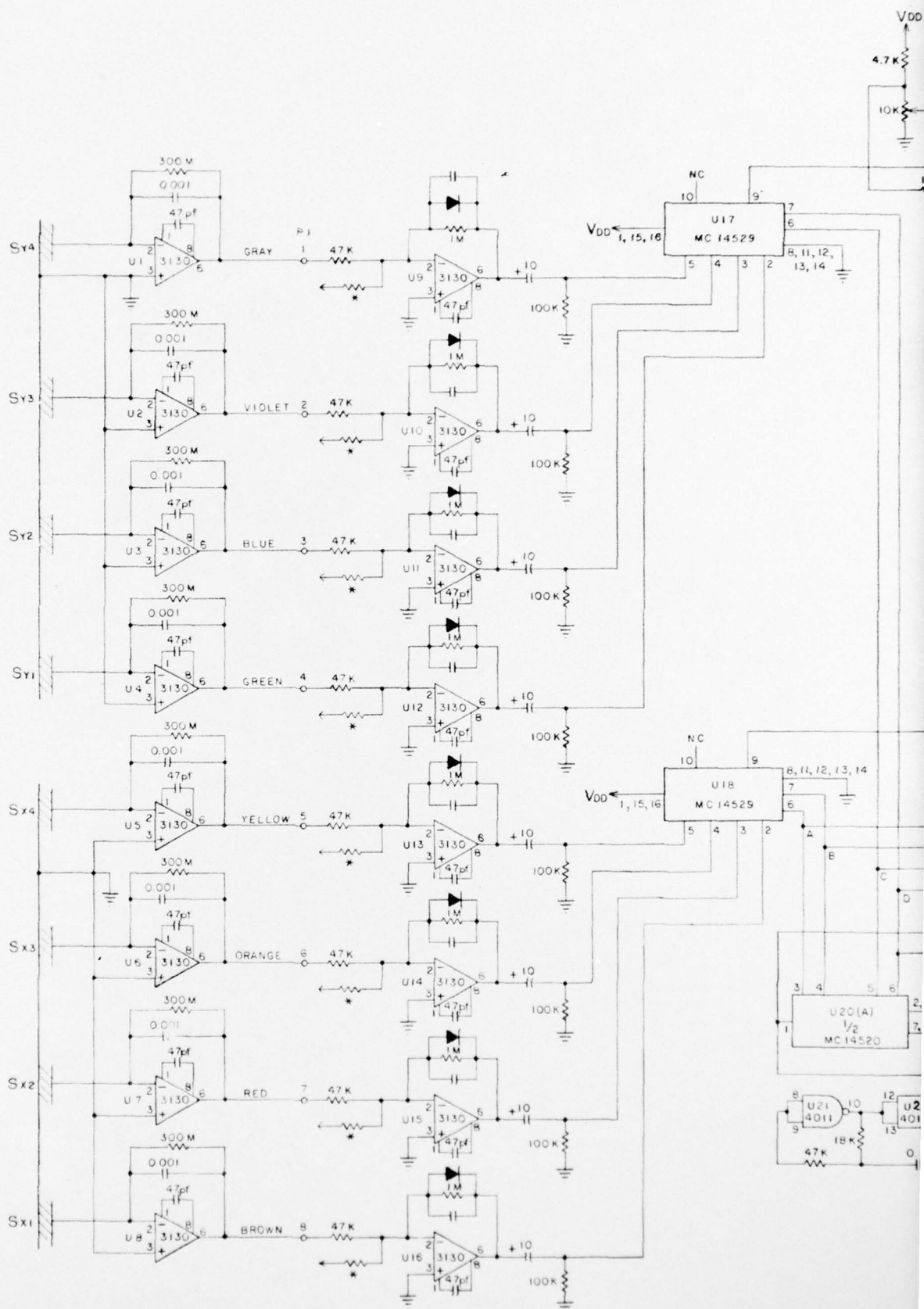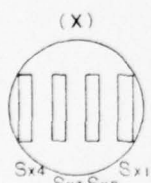
(1)   Signal Circuits

Figure 12 shows a complete schematic of the analog and digital circuits used in the infrared imaging detector and display. Each pyroelectric element in the sensor arrays has its own charge amplifier (U1-U8). The combination of a 0.001 mfd capacitor and a 300 megohm resistor as the feedback elements in the charge amplifier (RC=0.3 sec.) gives the amplifier a low frequency response with the corner (-3 dB) at about 0.5 Hz.

The post amplifiers (U9-U16) give the signal from the charge amplifiers an additional gain of 212 (47 dB). The diode in the feedback limits the voltage excursion to positive signals. A 10 mfd capacitor on the output of each post amplifier couples the amplified pyroelectric signals to multiplexers U17 and U18.

The multiplexers are addressed by a binary sequence on pins 6 and 7. As the 4 bit counting sequence progresses, detector element S_{x1} will be connected in one channel while S_{y1}, S_{y2}, S_{y3} and S_{y4} are scanned on the other. The counting sequence then addresses element S_{x2} while all y elements are again scanned. This multiplexing sequence continues until all 16 combinations of detector outputs are implemented and then the sequence repeats.

The outputs of the x and y multiplexers are coupled to the non-inverting inputs of comparators U19(A) and U19(B). The inverting input of each comparator is set to a positive voltage determined by potentiometers $V_{ref}(x)$ and $V_{ref}(y)$. Under a no target (no signal) condition, the reference voltages on the computer inputs keep the comparator outputs at zero volts or a logic LOW. If a target with sufficient radiant energy comes into the field of view of the instrument, analog voltages are generated which exceed the V_{ref} on the comparators. This signal causes one or both of the comparators to transition from a LOW to a HIGH state. When this occurs simultaneously on both comparators, a NAND gate combining the two outputs will transition from a HIGH to LOW. As the multiplexing binary sequence progresses as described above, a serial stream of digital data is generated on the output of the NAND gate, its character being a function of the thermal state of the field of view and the pyroelectric detector elements.

The output of the NAND gate is filtered using a passive RC low pass network to smooth the multiplexing transients. After inversion (U22)   the digital signals are combined with
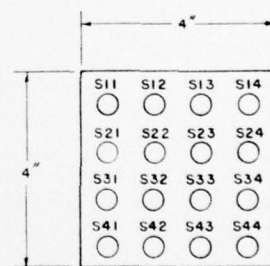
FIGURE 12. CIRCUIT
DETECTOR AND D

NOTES :
1. ALL DIODES 1N914 UNLESS OTHERWISE NOTED.
2. ALL CAPICITORS IN MFD UNLESS OTHERWISE NOTED.
3. "∗" SELECTED TO ADJUST ES OFFSET CONNECTED
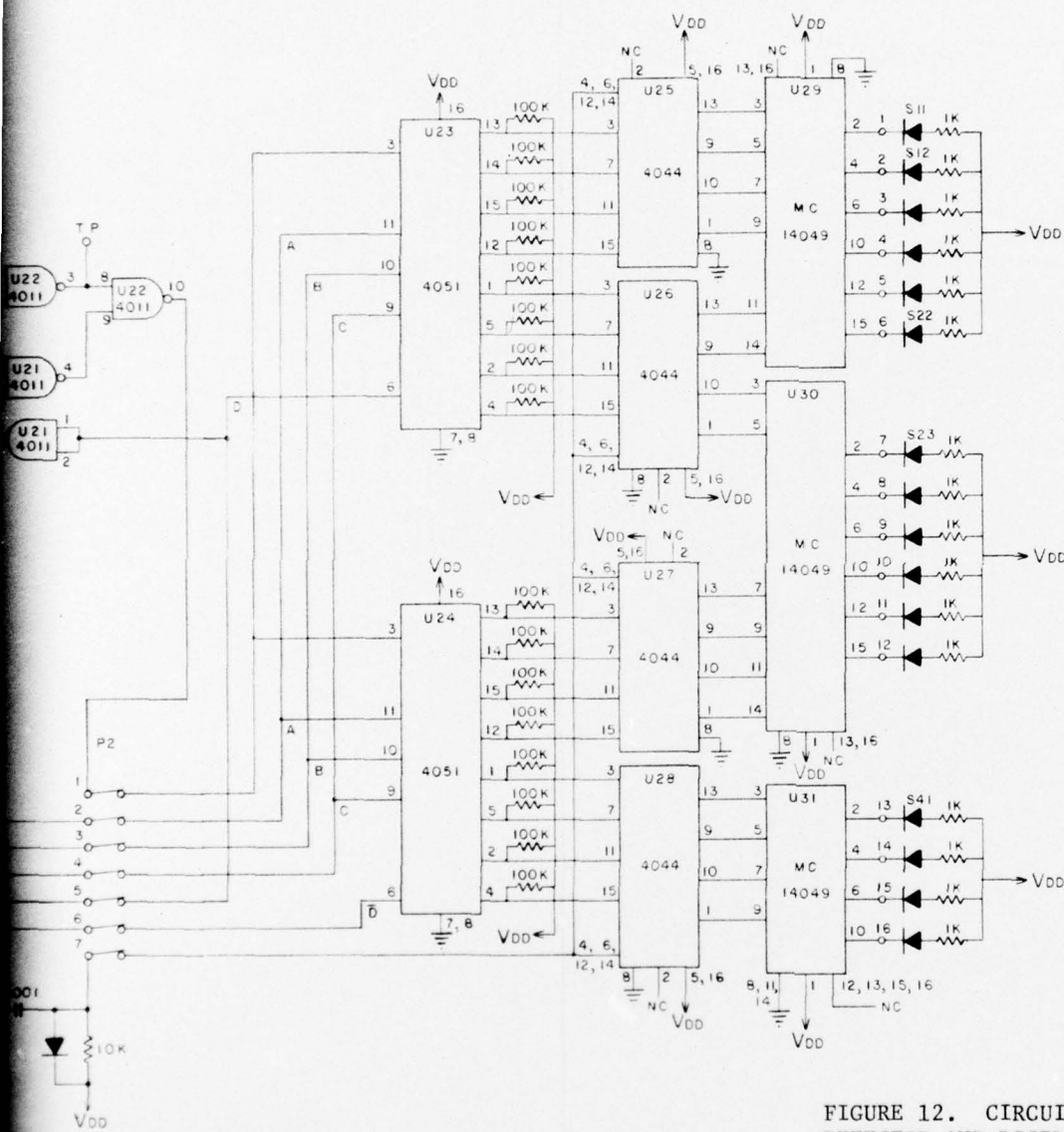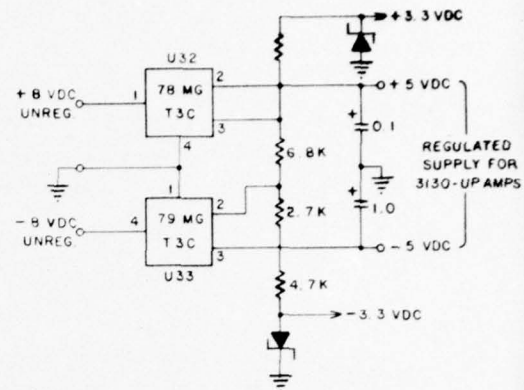   TO (+) OR (−) REGULATED SUPPLY.

FIGURE 12. CIRCUIT DIAGRAM FOR INFRARED IMAGING
DETECTOR AND DISPLAY

37

Since the outputs of the latch circuits
do not have the current drive needed to interface to the LED display,
an inverter/buffer stage (U29, U30, and U31) is used to furnish the
necessary drive to the output. The 16 signal lines are coupled to
the display board via a 16 pin DIP socket. The LED's which are
connected with their anodes to the unregulated supply through current
limiting resistors, are turned on by a LOW on the buffers.

3.   Operating Instructions-IR Imaging Detector

The breadboard for the IR imaging detector is
mounted in an enclosure equipped with feet for operation on a flat
surface (Figure 13). The bottom plate of the instrument is also
tapped for mounting on a conventional tripod.

Charge
Amplifiers

Polyethylene Window

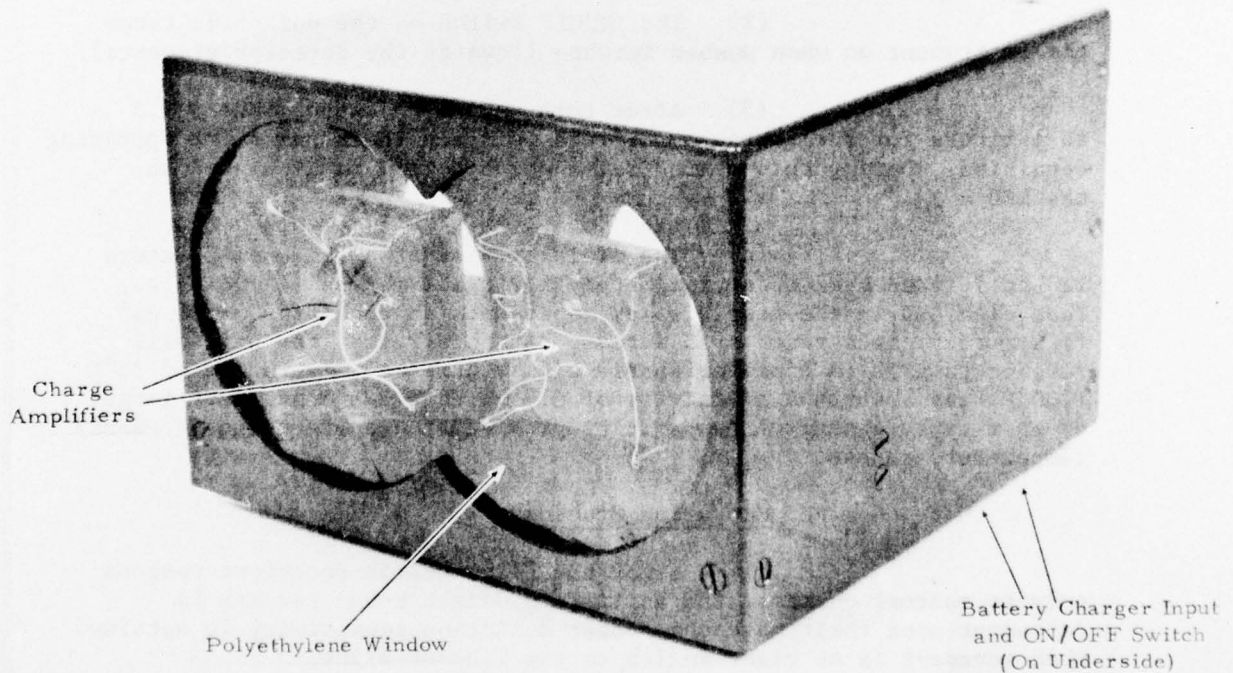Battery Charger Input
and ON/OFF Switch
(On Underside)

Figure 13.   Front View of the I.R. Imager.   The Rear Side
of the Charge Amplifier Housing may be Seen Through the
Polyethylene Window Covering the Viewing Entrance

39

a. Controls and Receptacles

Power ON/OFF Switch: Connects DC power to the instrument. When in the off position, the batteries are connected to the charger jack.

Charger Jack: Used for connecting the battery charger to the internal rechargable batteries.

X and Y Thresholds: Screwdriver adjustments for setting the DC threshold on the comparators.

LED Display - The rear of the unit is supplied with a 16 element LED display. These elements turn on in response to a moving, warm target within the field-of-view of the instrument.

b. Turn On Procedure

(1)   Set the instrument on a flat surface or mount it on a tripod. If placed on a flat surface, unit should be near the edge to prevent blockage of the field-of-view.

(2)   The ON/OFF switch on the underside turns the instrument on when pushed forward (towards the detector elements).

(3)   After turn on, allow approximately 0.5 to 1 minute for the charge amplifiers to reach their quiescent operating condition. During this period false outputs will be displayed on the LED's.

(4)   The field-of-view at a range of 3 meters (10 ft.) is an area of approximately 1.2 x 1.2 meters (4 x 4 ft.). Thus each LED in the rear display represents an area of 30 x 30 cm^2 (1 x 1 ft.^{2}) at a range of 3 meters. At this range, the unit will respond to a 10 cm diameter sphere with a surface temperature of 38°C (100°F) and a surface emitsivity of 0.95. To see a stationary target of this type, a shutter needs to be provided to generate the necessary temperature change.

c. Operating Procedure

(1)   Since the pyroelectric detectors respond only to thermal changes, the ability to detect human targets is dependent upon their movement. Best detection sensitivity is obtained when movement is at right angles to the line-of-sight.

(2)   Tests have shown that the unit is capable of detecting a human at distances greater than 5 meters (17 feet).

40

(3)   Since the detector elements are piezo-electric as well as pyroelectric, a moderate amount of vibration or movement of the instrument can generate false outputs. Initial tests, however, have not indicated this sensitivity to be a problem. The unit is more responsive to pressure fronts as might be generated by the opening of a door in an enclosed room.

(4)   The unit draws a quiescent steady-state current of approximately 100 ma. With a moderate amount of target activity, the unit will operate for 1 to 2 hours continuously.

(5)   The battery pack consists of 12 type CF400 Nicad rechargeable cells having a 500 mah capacity. The batteries may be charged at a high rate of 50 to 170 mA. According to the manufacturer, occasional overcharging for up to three days at these rates will not adversely affect cell performance. To charge cells at the slow rate and to maintain a fully charged cell, charge at 17 to 50 mA. The instrument is shipped with a battery charging lead with a series 27 ohm, 1 watt series resistor to limit the current to approximately 150 mA when connected to a 22 VDC power supply. The ON/OFF switch on the unit must be turned to OFF to connect the charger input to the batteries.

4.   Maintenance

a. General

The instrument is completely solid state, and little or no maintenance should be required under reasonable operating conditions. An accumulation of dirt or moisture on the transparent window or internally on the optics or the detector, can cause a loss of sensitivity for the instrument. The top cover provides protection against contamination and should only be removed when necessary.

b. Trouble Shooting and Alignment

(1)   The cover may be removed by loosening the two zeus fasteners on the bottom of the case. In removing the cover, extreme care should be exercised to avoid contacting the supporting elements for the charge amplifiers and the pyroelectric detectors (Figure 14).

(2)   If inoperable, the instrument should be first checked for charged batteries, obvious broken connectors, improperly seated plugs, improperly seated integrated circuits or gross optical misalignment problems. The open circuit voltage across the charge terminals should not be less than about 14 volts.
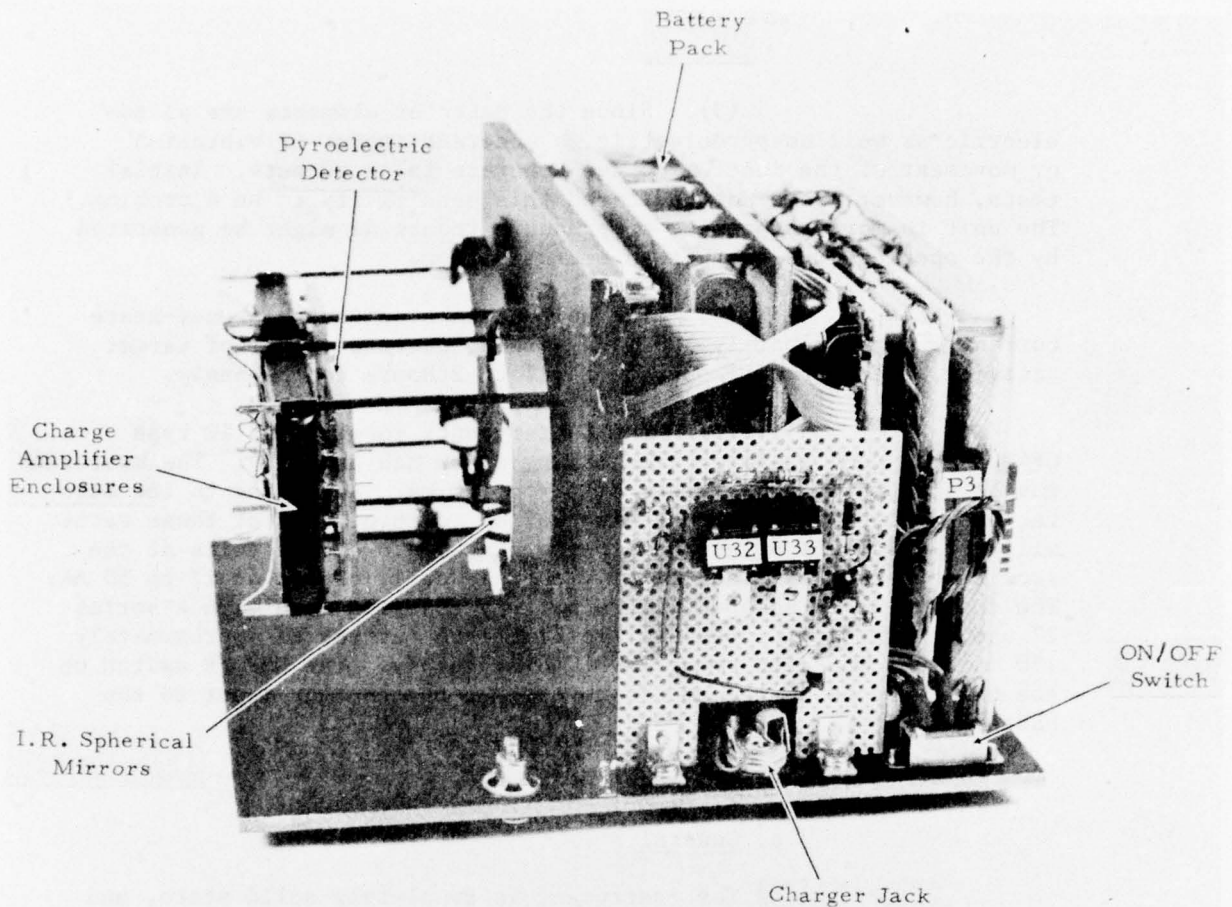
41

Battery
Pack

Pyroelectric
Detector

Charge
Amplifier
Enclosures

U32 U33

P3

ON/OFF
Switch

I.R. Spherical
Mirrors

Charger Jack

Figure 14. Side View of Instrument with Cover Removed

(3) A complete circuit diagram is furnished
(Figure 13) to aid in trouble shooting. The active circuits and plugs
have been assigned a component number and may be located on the board
with the aid of the pictures shown in Figures 15(a) and 15(b).

(4) With the exception of the detector elements,
all the electrical components are standard parts and can be obtained
from the respective manufacturers. Most of the integrated circuits are
available from more than one manufacturer.

(5) The PVF_2 pyroelectric elements are mounted
on the rear of the charge amplifier enclosures, facing the gold plated
mirrors. These elements should not be touched with the fingers or
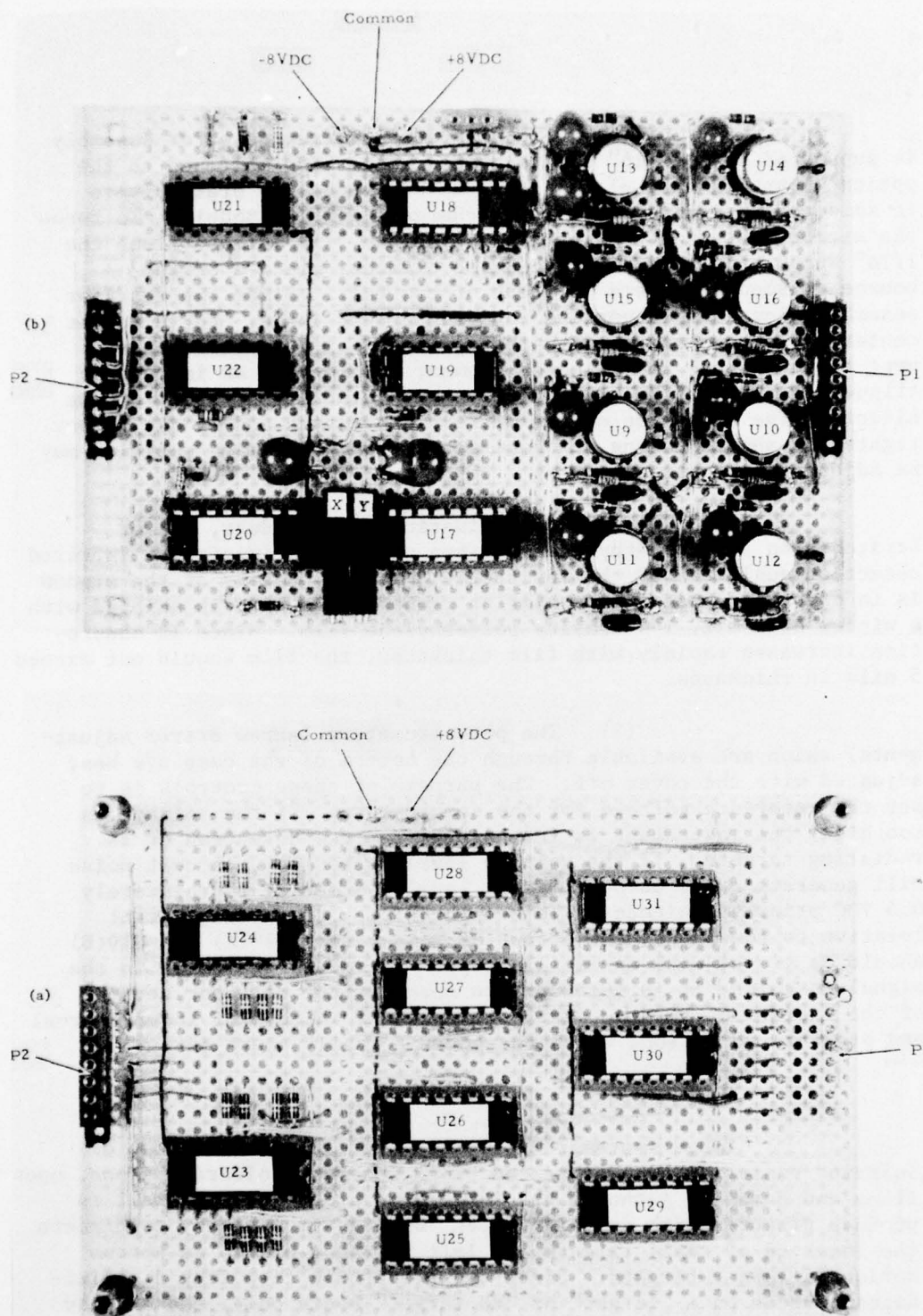contacted with mechanical devices such as test leads, etc.

42

Figure 15. Circuit Boards for IR Imager

43

(6)   Each charge amplifier/detector assembly is supported by 4, 1/16" square hollow brass rods fastened to the optical mounting base plate. A 3/32" square hollow brass sleeve is soldered to each corner of the charge amplifier module. To focus the mirror, detector combination, slide the 3/32" sleeve along the 1/16" supporting rods. To focus the element, place a bright source at about 5 meters in front of the unit. Slide the detector assembly along the supporting rods for a best image. For a target centered in the field-of-view the reflected image should appear near the center of the detector element. To center an improperly aligned image, use the nylon screws which contact the front of the mirrors. The back side of the mirrors are curved and by the proper tightening and adjusting of these set-screws, the image position may be adjusted.

(7)   Contamination such as dust, oil or scratches on the polyethylene entrance window may impair the infrared detection qualities of the instrument. If the quality of the window is in doubt, replace with a similar window. The unit is shipped with a window of 2 mil, low density polyethylene film. Since IR absorption increases rapidly with film thickness, the film should not exceed 5 mils in thickness.

(8)   The potentiometers (screw driver adjustments) which are available through the bottom of the case are best adjusted with the cover off. The purpose of these controls is to set the reference voltage for the comparators. If the voltage is too high, the instrument is insensitive for the detection of IR radiating targets. If the voltage level is too low, circuit noise will generate false outputs. This level was set at approximately 0.5 VDC prior to shipment. To see the effect of the adjustment relative to the input, the output of comparators U19(A) and U19(B) should be viewed with an oscilloscope. To reduce the noise in the signal circuits, it is necessary to cover up the detector section of the instrument with a tight fitting cover which will lower thermal and pressure variations which the cover normally keeps out.

Test Results

Image system tests were performed using sources of infrared radiation such as heated black spheres, soldering irons, open flame and humans. Although the 16 element array was too small to produce pictures with any significant detail, it was easy to discern the location of small targets and left to right or top to bottom motion of larger targets. Since the electronic circuitry discriminates sources on a "target" or "no target" basis only, the display does not present gray scale type information or relative intensity of the source.

The maximum range for detecting a human walking at right angles to the line-of-sight was 5.33 meters (17.5 ft.). For this test, the subject walked by at a normal walking pace.

At a range of 3 meters, a 10 cm diameter blackened sphere at a temperature of approximately 55°C (131°F) was used to map the field-of-view for the system. This spherical target was small enough to light only one LED sensor at a time. To see the sphere, a shutter was used in front of the sphere to generate a temperature change. The shutter consisted of a square piece of cardboard at the end of a 1 meter stick. After interposing the shutter in front of the sphere for 10 seconds, it was quickly moved away at right angles to the line of sight. Concurrent with this, the signal pattern on the LED display was observed. By moving the sphere to different x-y coordinates at a fixed range from the instrument, the spatial sensitivity of the system was mapped. The resulting data showed that the field of view at 3 meters was approximately 4 ft. by 4 ft. with some aberation distortion due to the spherical surface of the reflecting mirror. A spherical surface is inexpensive to polish but is only an approximation of the proper surface for focusing parallel light to a point.

At a range of 3 meters, it was possible to detect the 10 cm black sphere when it had cooled to 38°C (100°F). The ambient temperature during the test was 25°C (77°F). The radiant emittance for this sphere calculates to be ($\epsilon=0.95$)

$$W' = (0.95)(311)^4(\sigma)$$

$$= 504 \text{ watts/m}^2$$

From equation 29, the total radiant flux incident upon the mirror is

$$P = \frac{(.00785)(1.06 \times 10^{-3})(504)}{(\pi)(3)^2}$$

$$= 1.483 \times 10^{-4} \text{ watts}$$

The comparator thresholds during these tests were set at 0.5 volts. The signal voltage, between the charge amplifier output and the comparator input, is amplified by a factor of 213. Thus, to exceed the threshold of the comparator input necessitates a signal of 2.35 mV on the output of the charge amplifiers. A 2.35 mV output corresponds to a detector element generated current of 2.35 $\times 10^{-12}$ amps. Using this output to calculate a current response for the device gives

$$R_I = \frac{2.35 \times 10^{-12} \text{ amps}}{1.483 \times 10^{-4} \text{ watts}}$$

$$= 1.58 \times 10^{-8} \text{ amps/watt}$$

45

H. Piezoelectric Film Studies

At the outset of this project it was anticipated that approximately half of the effort would be applied towards the investigation and optimization of the piezoelectric effect. During the past year, however, much commercial effort has been applied towards this objective and low cost fabrication of the films. For instance, the Kuerha Corporation is now marketing sheets of PVF_2 piezoelectric film. For this reason a larger amount of the effort was directed towards the investigation of the pyroelectric effect of the films. The following paragraphs describe a piezoelectric phenomena which was observed and investigated.

A piezoelectric effect was observed in PVF_2 insulated pieces of hookup wire. A roll of wire (Alpha No. 5951) was purchased to test this phenomena and to make sensitivity tests.

The wire was poled by wrapping it around a glass cylinder which in turn was immersed in a beaker of saline solution. The insulated wire thus served as one electrode for the poling voltage, and the saline solution surrounding the insulation, the other electrode. The entire apparatus was placed inside a controlled oven to maintain the poling temperature at 100°C. Ancillary wires leading to the beaker coupled the high voltage power supply to the test element. PVC tubing with a series pump was used to circulate the saline solution between copper tubing in an external cool water holding tank and the poling beaker. The purpose of this heat exchanger type apparatus was to accelerate the rate of cooling for the saline solution. This cooling hardware when used reduces the length of time that the poling voltage must be maintained across the PVF_2 element and decreases the probability of a voltage breakdown.

The procedure followed for poling this wire was to heat the wire and associated poling apparatus to 100°C, apply the poling voltage for a duration of 10 minutes, then rapidly cool down the wire with the voltage still applied until a temperature of 38°C or less is reached. The 800 volt poling voltage used was determined empirically to be the maximum usable potential which could be maintained without causing a premature voltage breakdown in the insulation.

To examine the wire, thus poled, a test apparatus was designed and constructed which allows sensitivity comparisons between a variety of test wires and cable which had been optimized as vibration-sensitive line transducers using an electret material as the key element.

The 12-inch wire to be tested was stretched between clamps on the main frame of a test jig designed for this purpose. At the midpoint of the wire, a speaker driver was deflected by a sinusoidal input voltage. As the driver was moved about the rest position, the wire was stretched causing a piezoelectric voltage generation. This voltage was amplified using a high impedance amplifier with a gain of 40 dB. The input deflection was measured using a linear potentiometer attached to the shaft of the driver. The sensitivity of the element was calculated as the voltage

output divided by the displacement. All tests were run at a constant frequency of 5 Hz. To make contact with the outer surface of the insulated wire, a thin strip of copper clad mylar coated with silver epoxy was stretched adjacent to the wire.

The results of this testing showed that the most sensitive element was a piece of PVF_2 insulated wire which had been heated in an uncontrolled manner using a hand held heat gun, poled with 2.5 kV voltage and then cooled rapidly using bottled CO_2. The wire which was poled under controlled conditions as described using the saline solution had a response which was about 14 dB below the heat gun poled sample. Comparing a sample of wire with no conditioning to the controlled poling sample showed very little difference in sensitivity. Similar tests were also run on a commercially prepared sample of electret coax cable. The results of the electret coax cable compared to the response of the carefully poled sample showed very little difference in sensitivity. Thus it would appear from this test that higher fields are desirable in optimizing the piezoelectric characteristics and that the naturally occurring piezoelectric properties of the insulated wire are comparable to the electret cable.

In general these test results were somewhat erratic and showed no clear cut trends. It appears, however, that a sensitive element such as this could be useful for certain intrusion applications and the effect merits further investigation.

REFERENCES

1. This reference will be made available to qualified military and government agencies on request from RADC (OCDS) Griffiss AFB NY 13441.

2. T. Kovattana, et al., "Intrusion-Detection Devices and Systems for Air Base Security," Prepared for Rome Air Development Center by Stanford Research Institute, No. RADC-TR-73-246, (August 1973), AD 769 081.

3. This reference will be made available to qualified military and government agencies on request from RADC (OCDS) Griffiss AFB NY 13441.

4. Robert J. Phelan, Jr., et al., "High D^* Pyroelectric Polyvinyl-fluoride Detectors," Applied Physics Letters, Vol. 19, No. 9, (1 November 1971).

5. J. G. Bergman, et al., "Pyroelectricity and Optical Second Harmonic Generation in Polyvinylidene Fluoride Films", Appl. Phys. Letters, Vol. 18, No. 5, 203-205, (1971).

6. A. M. Glass, et al., "Pyroelectric Properties of Polyvinylidene Flouride and Its Use for Infrared Detection", J. Appl. Phys., Vol. 42, No. 13, 5219-5222, (1971).

7. A. Peterlin and J. Elwell, "Dielectric Constant of Rolled Polyvinylidene Fluoride", J. Materials Sci., Vol. 2, (1967).

8. A. Peterlin and G. Meinel, "Thermodynamic Properties of Drawn Linear Polyethylene", J. Appl. Phys., Vol. 36, (1965).

9. J. H. McFee, et al., "Pyroelectric and Nonlinear Optical Properties of Poled Polyvinylidene Fluoride Films", IEEE Trans. Sonics & Ultrasonics, Vol. SU-19, (1972).

10. G. Pfister, et al., "Pyroelectricity in Polyvinylidene Fluoride," J. Appl. Phys. (USA), Vol. 44, No. 5 (May 1973).

11. G. W. Day, et al., "Effects of Poling Conditions on Responsivity and Uniformity of Polarization of PVF Pyroelectric Detectors," Applied Physics Letters, Vol. 24, No. 210 (15 May 1974).

MISSION
of
Rome Air Development Center

RADC plans and conducts research, exploratory and advanced
development programs in command, control, and communications
(C^3) activities, and in the C^3 areas of information sciences
and intelligence. The principal technical mission areas
are communications, electromagnetic guidance and control,
surveillance of ground and aerospace objects, intelligence
data collection and handling, information system technology,
ionospheric propagation, solid state sciences, microwave
physics and electronic reliability, maintainability and
compatibility.